Dear Editor, Reviewer 1, Reviewer 2 and Reviewer 3,

Thank you all for taking so much time to provide your meaningful and insightful comments and suggestions. We have taken them all into serious consideration and have strived to work hard to address them point-by-point in this response, your original comments are given (unedited) in yellow highlight, our responses are given in blue highlight and updates to the paper *are given in italics*. Thank you again for your time and deep insights! With your support and nudging, we believe that the results will make both a meaningful and important contribution to the academic discourse. Many thanks again!

Best Regards,

Jason Cohen

ACP, July 2020
Review of Wang, Cohen, Lin, and Deng,

Constraining the relationships between aerosol height, aerosol optical depth, and total column trace gas measurements using remote sensing and models

Overall, this paper includes a novel idea of incorporating CO and NO2 column-concentration measurements, as well as CO/NO2, in a statistical regression approach to modeling plume rise. They input MOPITT CO, and NO2 from the OMI instrument, and use MISR aerosol data for model validation.

Thank you very much. This was our intention from the start with this paper, and you have summarized this point very well. If we need to make any bullet points about its importance or impact, we will use your wording, if it is OK with you.

However, the paper needs work, in my opinion. There are a few overall considerations that might warrant further attention, and some smaller technical issues; key points are given below.

I believe it is important to point out that this review is based on the originally submitted paper, not the highly edited version which the initial two reviewers re-reviewed. For this reason, it has taken a bit more time to carefully address the changes, since some were already previously changed. However, due to the important recommendations provided, I am trying my best to address these points in full. Please excuse anything which may have been missed.

Top-Level Notes:

Greater care is needed in separating background aerosol, including aged smoke and pollution, from smoke emanating from specific fires. Note that “pollution” often indicates anthropogenic origin, whereas the term appears to be used here to include aged (and possibly also some fresh) fire emissions, as well as background emissions from other sources. It would be helpful to make clear what definition

is being used, and to make a distinction between fresh emissions (the target of the modeling here) and background emissions, either from earlier fires or from other sources.

We have analyzed both the loading of the NO_2 column measurements and the ratio of the NO_2/CO column measurements over both those sites which only have measurements available of FRP and overall over the larger regions (Table S2). From these results, we find a few pieces of information. First, that the results are very similar in terms of the NO_2/CO column ratios over both those specific points containing measured FRP values, and those points within the fire plumes as a whole. This is an indication that there is not a significant amount of urban emissions of NO_2 found in any of these regions at least from a statistically relevant point of view. If there were, the NO_2/CO ratio would rapidly diverge between these approaches, due to the much faster chemical titration of NO_2 compared to CO. Second, we find that in general the ratio of NO_2/CO falls into three separate ranges (defined by the central 80% of the pdf). The first group (Siberia and North China & Central Canada) range from $1x10^{-4}$ to $9x10^{-4}$, the second group ranges from $2x10^{-4}$ to 15 $x10^{-4}$-$20x10^{-4}$, and the third group (South America) ranges from 6 $x10^{-4}$ to $43x10^{-4}$. This is a strong indication that the ratio of NO_2/CO is representing a physical meaning, possibly connected with the dryness and flaming fraction, the temperature of burning, the type of biomass being burned, etc. Furthermore, we find that separating the data into the high and low NO_2/CO ratio values and then comparing the PDFs of the MISR height distribution and modeled height distributions leads to a clear improvement of the regression model as compared to the plume rise model (Figure S7). We have added the following to the paper in three different locations.

On top of this, the NO_2 column loading and the ratio of the NO_2/CO column measurements over only the selected grids which have available of FRP measurements, and over the larger regions as given in Figure 5 are found to generally be consistent, with the ratio found to be more so (Table S2). This indicates the NO_2/CO column ratio over the fire regions tends to be consistent with the fire plumes as a whole, and is not found to be significantly influenced by urban sources of NO_2, which would lead to a vastly faster chemical titration of NO_2 compared to CO.

Following these ideas, the idea of characterizing the by the ratio of NO_2/CO is found to nicely separate the data into three different groups, based on the bands generated by the central 80% of each respective region's NO_2/CO pdf. Group 1 consisting of Siberia and North China & Central Canada, has a NO_2/CO range from $1x10^{-4}$ to $9x10^{-4}$. Group 2 consisting of the remaining regions, has a NO_2/CO range from $2x10^{-4}$ to 15 $x10^{-4}$ to $20x10^{-4}$. Group 3 consisting of South America, has a NO_2/CO range from 6 $x10^{-4}$ to $43x10^{-4}$. This strong differentiation is consistent with the ratio of NO2/CO representing a physical meaning, but being a single, continuous variable connected with the temperature of the burning, the wetness of the burning material, the latent heat flux, and the type and amount of biomass being burned.

… "under all conditions, and even more so at the respective top and bottom 10% of each respective range of NO_2/CO ratio, in which the subset of regression model heights performs much better than the respective plume rise model heights when compared with the MISR height distribution (Figure S7)"

Contributing to the issue of distinguishing sources, burning conditions often produce many small fires, possibly in addition to a few large ones. These might be difficult to represent accurately in a model.

This point is well taken. In the data we have used, we only have access to a single FRP value to represent the state of the total amount of fire within each pixel. Whether this single FRP value is due to many small fires found within that pixel, or a single large fire, we cannot distinguish. However, the vertical and horizontal meteorological measurements, such as wind and temperature are also derived from larger-scale average values, frequently 10s to 100s of km in size. The column measurements of OMI and MOPITT are also coarser than the FRP measurements. There is a good reason for this, because in the real atmosphere, small scale turbulence and mixing will impact smoke emitted from the fires, and cause them to merge. These assumptions of scale are built into the plume rise models themselves are based on the thermodynamics of the system, as compared to the eddy-scale dynamics. For these reasons, the overall results are not expected to be any better using higher resolution measurements unless they are guaranteed to be accurate, and unless an eddy resolving model is used. However, presently there are no remotely sensed measurements available to match the required spatial and temporal scales. Therefore, we have assumed that the data given within each pixel is distributed into a single fire (in the case of FRP) or is evenly distributed (in the case of wind speed and direction, temperature, and remotely sensed measurements).

Addressing this point, we have decided to look at the measured plume rise heights and model values associated with the top 5% of measured FRP values (FRP>132W/m2) as well as the bottom 5% of measured FRP values (FRP<8.5W/m2). Overall, we do observe that both the measured and modeled mean plume rise is slightly higher for the very high FRP values than in the case of the very low FRP values, as expected. Furthermore, we notice that there are more plumes found above the boundary layer in the measurements corresponding to very high FRP values than in the case of very low FRP values, although there still are plumes over the boundary layer in both cases. This is where there is a considerable amount of value added from using the regression models that include the remotely sensed measurements of NO_2 and CO, as compared to the plume rise model.

The following have been added to the paper:

Analyzing the extremes of the FRP, leads to a top 5% of measured FRP of 132W/m^2 and a bottom 5% of measured FRP of 8.5W/m^2.

The high end of the FRP range of the observations in this work is not considered to be very hot in terms of fires, which should in theory help to reduce the known plume rise model bias of underpredicting very

strong FRP conditions, leading to an overall improvement in the plume rise model as analyzed in this work, as compared to when it is less constrained. As expected, there are more plumes found above the boundary layer in the measurements corresponding to very high FRP values than in the case of very low FRP values, although more importantly, there still are plumes found over the boundary layer in both cases, which is not expected based solely on the plume rise model formulation.

Also, there are limitations in the degree to which the remote sensing instruments can resolve structure in the boundary layer (MISR plume-height uncertainty is between 250 and 500 m), and models are notoriously poor in simulating boundary layer height and vertical mixing timescales. So there are plenty of possible reasons why discrepancies between the "observed" and "modeled" boundary layer results might occur.

This is an important point to make. We have carefully re-analyzed the data (as presented in Figure S2) and determined that other than in Alaska, the differences between the MISR measurements, the plume rise measurements, and the regression model measurements in the boundary layer are always more than the 250m to 500m uncertainty range of the MISR measurements, meaning that the results as given in the other regions are consistent with the conclusions and assertions made. This said, your point about the uncertainty of the MISR measurements in the boundary layer is extremely important, and we have added more details to the text to address these measurement uncertainties that exist within the boundary layer.

The only region over which the finding may not be statistically relevant is in Alaska, where the difference between regression measurements are all constrained to within a 500m height band, which falls into the MISR measurement uncertainty measurement range.

Many 1-D plume rise models tend to overestimate injection heights for low plumes and underestimate them for higher plumes, thus diminishing the range of simulated height variation.

This observation of overestimating low FRP plume rise heights and underestimating high FRP plume rise heights was found in our own previous work as well (Cohen et al., 2018), and was one of the motivating reasons behind this present work.

As can be observed for our data (Table below), it seems that there basically are no conditions that exist for very high energy plumes in the first place (5% level is 8.5W/m^2, while the 95% level is 132W/m^2). This hence should negate the plume rise model's known tendency to underestimate higher plumes.

We believe that this point has already been addressed by the previous changes to the manuscript found above.

With a closer analysis of the reasons CO and NO2 column concentrations improve the correlation with plume height in regression models, the current paper might shed some specific light on this issue.

It appears that for the third group (the highest NO_2/CO ratio group) that the regression model works much better than the plume rise model, even at the extremes of the distribution. In some of the cases for group 2 (the moderate NO_2/CO ratio group) that the regression model works considerably better than the plume rise model, even at the extremes of the distribution. This indicates that under conditions that produce more NO_2 (i.e. hotter conditions) or that produce less CO (i.e. more oxygen deprived conditions) that the model works better in general (i.e. the overall mismatch with MISR is reduced). Overall the improvement is that the low biases are reduced, while the ability to reproduce a larger fraction of the plumes over the boundary layer is also increased.

We have already made changes to the text to address this issue.

Detailed Notes:

1. The references used in the **introduction** are a bit off. Although they are relevant to the subject of plume-height retrieval, many are cited in the wrong context. A few cases are listed here. The authors might go over all the cited references and assure they are listed in the appropriate context;

Thank you very much for your recommendations and deeper list of references. We have made the changes recommended and extended upon those to other similar parts of the work. The following details a point-by-point response.

1. For example, on Line 27, Val Martin et al. 2012 is about testing a plume-rise model using MISR plume heights, and Nelson et al. 2013 is about the MISR plume height algorithm. Yet they are referenced regarding "the impacts that aerosols have on clouds, radiation, the atmospheric energy balance, and climate, human health, and ecosystems..." Although plume-rise does bear upon all these, the papers referenced do not cover those aspects.

   Addressed. These references have been moved to a more appropriate spot and different references have been added in here.

2. Mims et al. 2010 (Line 29) is about plume-rise in Australia, not about the atmospheric energy budget. An aerosol transport model result would probably be a more appropriate reference than Winker et al. 2013 (Line 31) when talking about the atmospheric distribution of aerosols in general.

   Addressed. These references have been moved to a more appropriate spot and different

references have been added in here.

3. On Line 37, Vernon et al. (2018) should probably be Flower and Kahn (2017; doi: /10.1016/j.jvolgeores.2017.03.010). The Alaska plume-rise results (Lines 47-48) are in Kahn et al. 2008, not Kahn et al. 2007. Val Martin et al. 2018 (Line 48) is about the MISR plume-height climatology, and although it mentions CALIPSO, that is not the point of this particular paper. (Maybe the Winker et al. 2013 reference belongs there.)

Addressed. These references have been added, updated, and/or moved to a more appropriate spot, while suggested references have been added in here.

4. On Lines 51-52, the climatology of plume heights in Val Martin et al. 2018 shows that smoke is injected above the boundary layer frequently at high latitudes in summer, and in a few other geographic locations, but in areas where agricultural burning is prevalent, high injection is rare.

This point is clearly made and clarified.

5. On Line 58, Ichoku and Ellison 2014 actually derive emission factors to estimate smoke source strength; they do not assess plume-rise models – that might be Val Martin et al., 2012 and Paugam 2016.

Thank you very much again. Your deep insights have helped us to better give credit to where it is due, and helped us to organize the referencing for those who ultimately read this work.

6. And it continues... it is up to the authors to go through all the references.

We have continued to make additional changes, as marked in the paper itself.

2. Lines 74-75. “The vast majority of biomass burning is a man-made activity...” This is

true only in certain regions, not in general, and not globally.

We completely agree with the point about lightning induced fires, and have taken this into account in our edited version.

The vast majority of biomass burning in the tropics and non-tropical agricultural regions of the world is a man-made activity (Kauffman et al., 2003; Achtemeier et al., 2011; Paugam et al., 2016), while in certain arctic regions, lighting accounts for a significant amount of biomass burning (Generoso et al., 2007).

3. Lines 85-90. The primary reasons plume rise models have difficulty reproducing the

actual aerosol vertical distribution in the atmosphere is difficulty in quantifying the heat flux and in modeling entrainment (Kahn et al., 2007, Val Martin et al., 2012). Removal mechanisms in general, and rainfall in particular, are relevant to longer distance transport and deposition, but

not to plume rise in most cases. Aerosol processing in polluted conditions is important for aerosol chemical evolution but is likely to be a dominant factor in plume rise modeling only in very special cases. This entire paragraph discusses factors relevant to transport and deposition, without making clear that it is no longer discussing plume rise modeling.

We believe that one of the problems with the current approach to plume rise modeling is that it is not considering the anthropogenic heat profile and emissions correctly. For more optically thick, the added heat from BC absorption is more significant than previously considered, especially so in the tropics. In highly humid air, the heat due to condensation of water vapor into an associated aerosol water phase is large and also not considered by the plume rise models. We do agree that for relatively thinner plumes, in relatively drier atmospheric conditions, with generally larger heat loadings at the surface that your point is well taken, even though as we have pointed out here, within the central 90% of the data, we do not have any extremely high measurements of FRP. We just want to be fair about the fact that there are important aspects of the thermodynamics that are related to plume rise modeling, which have not been considered in traditional plume rise modeling. To make this point clearer, we have added the following sentence, following the reviewer's recommendation:

The present generation of models has difficulty to reproduce the actual vertical distribution of atmospheric aerosols when addressing cases that do not tend to have a combination of a highly energetic fire source, a relatively dry atmosphere, and a relatively optically thin smoke column emitted by the fire.

4. Lines 94-95. Again, the references don't seem to address the context. And it is not clear what type of simple models are being discussed (plume rise or transport and deposition).

We have inserted the words *plume rise* to make this clear.

5. Another paper that might be worth reviewing in the context of this study is Heald et al. 2004, doi:10.1029/2004JD005185. And the following might also be of help: Kahn 2020 doi.org/10.1029/2020EO138260.

Thank you for supplying these excellent works. The last sentence of the paragraph has been expanded, and now reads as follows:

In summary these factors can lead to actual changes in the vertical distribution of aerosols that simple models are not able to reproduce, including those which have used inverse modeling with a fixed vertical a priori (i.e. Heald et al. 2004; Cohen and Prinn, 2011), in turn affecting the distribution of aerosols hundreds to thousands of kilometers downwind, supporting new measurement-based perspectives (i.e. Kahn 2020).

6. Lines 129-133. Given the diversity of burning conditions in boreal forest, tropical forest, grassland, agricultural land, etc., it is not clear why one would look at global average variability rather than stratifying at least into these general categories.

Our findings seem to be that the NO_2/CO ratio is less dependent on the different land use types than it is on other factors, some of which are still not clearly known. We argue that from the

atmospheric perspective, and the perspective of the ultimate vertical distribution of the aerosols from fires, that the NO_2/CO ratio may be more important. It would be great to dig more deeply into these various driving forces in a future project. Thank you for the suggestion!

7. Lines 134-137. Rather than something deeper, the distribution of burning reported here seems to just reflect that the subtropics are dominated by un-vegetated desert.

Our work has found and analyzed regions in the subtropics including: Argentina, Southern Eastern Europe, and Northeastern China. However, it is true that urban emissions sources dominate in many of the subtropical regions, including in the USA, Central China, and Southern Europe. These regions may therefore be missed using the variance maximization approach, where the variation induced by fire emissions are masked due to random variations induced by the considerably larger urban sources. This insight just means that a new perspective will be required to adapt the finding here to regions which have a mixture of urban and fire sources, which for CO means very large areas, as its lifetime is relatively long.

8. Line 147. The reason given for averaging MOPITT to 1x1 degree does not seem to be justified by the statement that the data are affected by clouds and orbital limitations. MISR data are also affected by clouds, MISR is in the same orbit as MOPITT, and MOPITT actually has a wider swath, yet the MISR data are averaged to 10 x 10 km in this study.

CO is a much longer-lived species in-situ as compared to aerosols. Therefore, geospatial variance is much smaller due to chemistry and physics. Hence, such averaging has been shown to be reasonable. This may be a limiting rationale behind why it is hard to separate smaller fire sources from larger urban sources in the mid-latitudes. However, it has no impact on the results given in this work. Again, a very interesting thing to follow-up on with respect to the spatial and temporal resolution issues.

9. Line 158. Note that NO2 is produced by a range of anthropogenic activities, so as the focus here is on wildfires, one must be careful not to assign to wildfires NO2 produced by other sources.

Due to the higher spatial resolution of OMI and the much shorter lifetime of NO_2 as compared to CO, this is much easier to address. It is possible that there are some co-variations in the NO_2 emissions that correspond with the same temporal variation as the fires, but they are not found to make a significant impact in this work. However, the point is well regarded, and would lead overall to an underestimation of the spatial distribution of the overall fires discussed in this paper, with an example being the biomass burning of transported wood occurring in urban areas not be differentiable within this context. Perhaps an excellent follow-up work to look at in terms of upward looking AOD and NO_2 measurement platforms?

10. Lines 162-163. There are many other differences between wildfire emissions and those from urban combustion sources.

While there may be differences in the ratios of carbon, nitrogen, and oxygen between biomass and other urban combustion sources, these do not lead to such huge differences in the output emissions. The majority of the differences, with respect to CO and NO_2 emissions stem from the environment and/or way in which these sources are burnt. For example, biomass fuel cut from a

tree, dried out, turned to charcoal, and ultimately used for cooking may be quite similar to coal used for cooking, although one is biomass and the other is urban. The critical issue here is using the geospatial and temporal variations in the amounts and ratios of NO_2 and CO as measured, to attempt to understand the differences in the sources and the ultimate rise of the plume heights. A slight change will be made to the paper, so as to be slightly clearer with respect to the point about the environment in which the burning is occurring.

Although emissions from biomass burning are similar to those from urban combustion sources, there are two major differences, arising from the much higher burning temperature and the environment in which the combustion occurred.

11. Line 169-173. Note that the Freitas (2007) model was developed in part to address some of the limitations of the Briggs model. So was Sofiev et al. (2012, doi:10.5194/acp- 12-1995-2012), which probably should be contrasted with the approach given in Section 2.7 of the current paper.

This point is important. To address this issue, the last revision added an entire section on comparison against the MERRA reanalysis. This reanalysis uses a model which includes CAPE type of motions, and therefore would be similar in nature. This has already been explained in its entire own section, 2.8. A reference to Sofiev et al., 2012 is added.

12. Line 177. You might say more about the MODIS data used; "MODIS hot-spot information" is not enough.

This was addressed in the previous revision.

13. Lines 179-185. A key input to the plume rise model would be the dynamical heat flux, or some other measure of the buoyancy generated by the fire. As this would not come from the NCEP reanalysis, does this come in some way from the MODIS hot-spot information?

Yes, from the MODIS hot-spot information. This point was addressed in the previous revision.

14. Lines 223-224. Figure 2 is very difficult to interpret. The axes should be labeled, and the number of counts in each region should be given, maybe in the legend or in Table S1 (or both). Also, some smoothing or an expanded vertical axis might help in eliciting the main patterns from the mass of lines in this figure.

This change was made in the previous revision. It was divided into 4 separate plots and the axes were enhanced.

15. Line 225. An injection height of 29 km seems very unlikely. The most extreme PyroCb on record reached no more than 3-5 km above the tropopause, to about 17 km in that case. The extreme height seems more likely to be an error, perhaps in co-registration of the multi-angle images.

Point well taken. The following has been added:

(with extremely high values in the middle stratosphere possibly an error),

16. Line 231. If ~8% of the plumes in this study are above 5 km, and they are likely to be concentrated in certain regions, wouldn't that be important to include in the study, especially as these would have to be major events, possibly generating a disproportionate amount of smoke?

The newly revised lines, encompassing both the 2nd revision and your comments are given below. As you can see, the number of such very high plumes is very tiny.

Due to the fact that first, the majority of the plumes are injected into the boundary layer or the lower free troposphere, second that this paper is not looking into the underlying physics of stratospheric injection (Pengfei Yu et al., 2019), and third that plumes tend to accumulate within layers of relative atmospheric stability, therefore an upper bound cutoff on the measured values of 5000m is imposed. This is consistent with the fact that over the regions of interest in this work, fewer than 0.48% of the total plume heights are more than 5 km.

17. Line 240. The vertical resolution of the MISR plume height retrievals is between 250 and 500 m, so how does the data set report percentages of plumes below 200 m?

Thank you for raising this excellent point. Based on your knowledge of the data, we have adjusted these calculations to 500m, so as to ensure that plumes below the 24-hour boundary layer height are constrained based on both the daytime boundary layer height (which may be as low as 200m) and the measurement uncertainty. We have altered the text as below, including the new calculations:

To safely consider those plumes which are definitively near the surface (i.e. never above the boundary layer) a plume height below 200m would roughly corresponds to the boundary layer maximum in the middle of the day (Guo et al., 2019). However, due to the measurement uncertainty of the MISR heights being between 250m and 500m, instead the percentage of total plumes with a height below 500m is chosen, which is found to have a total percentage of respective plume heights of: global (11%) and a range from a minimum of 0.68% in Southern Africa to 49% in Argentina. Given the diversity of these results, there is a need to more deeply understand the driving factors across all of these different regions, as well as the importance of biomass burning in terms of transporting aerosols through the boundary layer.

18. Lines 244-253. Two limitations of the MISR data should be noted. First, as the MISR swath is about 380 km wide, locations on Earth are sampled on average about once per week, which still captures many fires, but misses many others. Second, the MISR overpass is at about 10:30 AM local time, whereas biomass burning tends to peak in the late afternoon. These limitations do not invalidate the work, but they should be taken into consideration when presenting global statistical conclusions. For example, the burning season might appear truncated if much of the actual burning occurs only later in the day than the MISR overpass.

We agree that pointing out clearly some of the limitations of the measurements only strengthens the results. However, as the co-author on a paper currently under review looking exactly at the time of day of overpass issue, I am not sure that I completely agree with your assessment that morning overpasses have a bias compared with afternoon overpasses, although in some regions

this seems to be the case. Regardless, we have added and/or changed the text in the following way, to reflect the limitations in the coverage from MISR.

Furthermore, MISR has a relatively narrow swath, not providing daily coverage to all points, coupled with a morning overpass time which may lead to negative bias in some regions and positive bias in other regions in terms of observed fires. This combination allows us to clearly demonstrate that the observed smoke peaks are in fact due to burning of a significant amount of material, and are true cases of biomass burning, while not possibly being fully representative of all biomass burning events. In the observed cases,

19. Lines 259-269. FRP is only loosely correlated with plume buoyancy, for specific physical reasons; the dominant ones are: (1) partly filled pixels; (2) non-zero smoke opacity above the fire front (which you mention), and (3) fire emissivity less than 1 (e.g., smoldering). This results in loose correlation between FRP and injection height. See, e.g., Kahn et al., 2007 or Val Martin et al. 2012, Figures 7 and 8 and associated text.

The point about partly filled pixels has been added and the references updated. The perspective taken by the plume rise models is that true fire radiative power should be strongly related to plume buoyancy at the surface, while these factors create a discrepancy between the true FRP and the measured FRP.

On top of this, there may be partially filled pixels in the remotely sensed measurements (Kahn et al., 2007; Val Martin et al. 2012).

20. Lines 283-284. Gas emissions are related not solely on the buoyancy generated. In addition to the factors mentioned, different ratios of CO and NO2, depend, for example, on fuel type and surface moisture.

This was already addressed from version 1 to version 2. Thank you!

21. Lines 294-300. Note that fire fronts are typically on much smaller scales (10s of meters) than the CO and NO2 measurements. In Northern China, high background CO and NO2 is likely due to anthropogenic activity, whereas in Siberia, it is likely from other fires. Often multiple fires of different sizes burn in an area where fuel load and fire weather conditions are favorable. You probably need to carefully separate any background contributions from those generated by the fire of interest to obtain a meaningful relationship between the gas concentrations and plume rise. Simply identifying above- background pixels and assuming the background contributions are negligible might not be good enough.

This important point was thoroughly addressed between version 1 and version 2. See figures 5 and S7.

22. Lines 323-328. Aerosol radiative effects, rainfall, etc., can be important for transported smoke, perhaps even a few hours after emission. But the buoyancy, ambient atmospheric structure, and entrainment are likely to dominate during plume injection.

This statement has been partially addressed between version 1 and version 2. Further support is

added to the text below.

This finding is consistent with evidence that the vertical plume rise and distribution of tropical convective clouds is sometimes dominated by in-situ heating and turbulence even more so than the initial heat of condensation (Gunturu, 2010).

23. Line 337. I've lost track of which plume rise model is being discussed here. I thought you were testing all seven regression models given in Equations 1-7.

In all cases, the plume rise model refers to the physical plume rise model, not Equations 1-7 (although Equation 7 is structurally similar to the plume rise model). The regression model, or Equation 1 to Equation 6 model (other than Equation 7) refers to the models based on the measurements of dynamical as well as remotely sensed measurements of NO_2 and/or CO.

24. Lines 352-355. Again, I'm unclear what model is being discussed. I do not recall discussion earlier of a plume rise model having a vertical resolution that would resolve better than 0.5 km in the boundary layer.

The plume rise model results frequently show a distribution of less than 500m, as demonstrated in Figure S2. This, combined with your information that the MISR measurements are uncertain from 250m to 500m is a motivating factor behind this work to better address the vertical height issue!

25. Lines 414-421. It is interesting that the column concentrations of CO and NO2 provide better correlation with plume height than FRP or wind. The CO and NO2 are not height- resolved, although in some cases these gases would be primarily generated by the fire in question, perhaps yielding an indication of fire intensity. It might be worthwhile to investigate this further, as it would offer a physical explanation for the observed correlations. Identifying the conditions when the relationship does not apply, perhaps cases where NO2 or CO from other sources dominates, for example, might also help in interpreting the data and improving the model.

This is a critical reason why we have used few of the locations in the extratropics. It is hard to find regions that we can be certain of, from a global analysis and perspective that are clearly dominantly influenced by biomass burning. It is hoped that this technique can be expanded by the community over specific regions using both high spatial resolution measurements from the new MISR products, TROPOMI, etc., or in addition with newer modeling efforts. We also look forward to attempting to further expand this work into areas which are more diverse in terms of their atmospheric background loadings.

26. Lines 435-437. Regarding the much smaller variance in the measured values, it might be worth remembering that the MISR plume heights are all acquired only around 10:30 AM local time.

The idea of a possible temporal mis-match was mentioned clearly before, as per your suggestion. It is quite interesting to note that MERRA does not provide the time information clearly, even though it is supposed to be assimilating the MISR data! We support your effort at clarity in this regard.

27. Lines 451-458. I think the reasons behind the performance of the regression model might be among the most important results of a study such as this one.

We appreciate this important point and have both edited existing text and added additional text to support this insight.

This is further found to be true in the case where the data at the high end of the NO_2/CO ratio profile are considered. This improvement is found in terms of both the bias and the RMS… These findings are consistent with real true world conditions, where there is a significant impact of co-emitted aerosols and/or heat, and these results with the NO_2/CO ratio would hint that higher burning temperature conditions, or fewer oxygen limited conditions, may be important driving forces.

28. Section 3.4. One way to assess regression model performance is by randomly selecting 10% or 20% of the data to leave out when the regression coefficients are calculated, and then comparing the model with against the withheld data.

We understand and appreciate this point. We also have found that the data is quite limited and may not be sufficient in some regions to begin with. Since this is a way to compare the regression model against its own fitting, and due to the lack of abundance of data, we feel that this exercise may be better suited to follow-up work analyzing the reasons for uncertainty behind these and other results. Thank you very much for this important point!

29. Lines 508-514. Accounting for the complex distribution of flaming and smoldering in many fire situations, especially larger ones, and modeling entrainment accordingly, are probably important if not dominant factors.

We feel that the reason why including the NO_2/CO ratio specifically may be so important is that it can help us evaluate from a different perspective the issue of total biomass consumed (a function of CO) versus the atmospheric temperature at the point of combustion (a function of NO_2). Perhaps this new approach will help us to move beyond just flaming and smoldering, into a more diverse way to look at this issue. We have added the following:

Thirdly, the finding that the NO_2/CO ratio is extremely important in terms of matching the vertical distribution works to address the larger community issue of flaming versus smoldering in a more smooth and precise way, opening the possibility of a new continuum approach to consider burning wetness, temperature, and heat.

The authors have provided a very complete and thorough response to my questions. Some of my questions originated from not being in the plume modelling field and I appreciate the authors working hard to explain what is going on and educate me. I commend the authors on such a thorough response, especially with current events as they are.

Very nice clear explanation of the plume model. I fully agree with the authors that simple models offer better insight in many situations because they aren't a black box.

Based on the additional explanation that the authors have provided on their formulation of the MLR I think their rationale makes sense. The added text is very helpful to readers such as myself to understand what each MLR is doing.

I appreciate the description of how the reanalysis has limitations in regions like the Andes, or when cloud cover is persistent. The authors' have clearly done a lot of work to make sure they understand what is going into making MERRA-2 work. I think the inclusion of the MERRA-2 data will be interesting to the NASA modelling community since it appears to work less well than the regression model. Modelling biomass burning is a known issue with MERRA-2 [Buchard et al., 2015] and evaluations such as this are important.

Overall I find the paper clear and improved and recommend acceptance.

Thank you very much for all of your support and deep insights throughout this entire process. We appreciate the fact that with your help, significant improvements have been made.

934: "Has difficulty in reproducing"?

This has been improved in response to a recommendation from the new reviewer. The new sentence is now:

The present generation of models has difficulty to reproduce the actual vertical distribution of atmospheric aerosols when addressing cases that do not tend to have a combination of a highly energetic fire source, a relatively dry atmosphere, and a relatively optically thin smoke column emitted by the fire.

1000/1023: "specifically"

This part has been corrected.

Pg 32 ln 065: Predictors in a regression model don't have to be orthogonal (https://www.statisticshowto.com/orthogonality/) or uncorrelated with each other. If the predictors are really strongly correlated it is a problem, but the authors are training and predicting on different data sets so it seems robust and I don't think they need to worry all that much. If the authors want to they could throw in a correlation matrix plot to show that the predictors aren't very strongly correlated, but I think that is unnecessary.

We agree with this observation. The strongest amount of correlation may be related to the overpass times, since the various measurements are all on the A-Train. But otherwise we do not observe any significant correlation, as demonstrated clearly in the new Figure 5.

Pg. 34 ln 143: ‘which is produced more’

This has been clarified. Thank you!

Buchard, V., A. M. da Silva, P. R. Colarco, A. Darmenov, C. A. Randles, R. Govindaraju, O. Torres, J. Campbell, and R. Spurr (2015), Using the OMI aerosol index and absorption aerosol optical depth to evaluate the NASA MERRA Aerosol Reanalysis, Atmos. Chem. Phys., 15(10), 5743-5760, doi: 10.5194/acp-15-5743-2015.

References

Achtemeier, G. L., Goodrick, S. A., Liu, Y., Garcia-Menendez, F., Hu. Y., and Odman, M. T.: Modeling Smoke Plume-Rise and Dispersion from Southern United States Prescribed Burns with Daysmoke, Atmosphere, 2, 358-388, doi:10.3390/atmos2030358, 2011.

Cohen, J. B. and Prinn, R. G.: Development of a fast, urban chemistry metamodel for inclusion in global models, Atmos. Chem. Phys., 11, 7629–7656, doi:10.5194/acp-11- 7629-2011, 2011.

Generoso, S., Bey, I., Atti, J.-L., and Bron, F.-M.: A satellite- and model-based assessment of the 2003 Russian fires: Impact on the Arctic region, J. Geophys. Res., 112, D15302, doi:10.1029/2006JD008344, 2007.

Gunturu, U. B.: Aerosol-Cloud interactions: a new perspective in precipitation enhancement, 2010.

Guo, J., Li, Y., Cohen, J. B., Li, J., Chen, D., Xu, H. Lin L., Jinfang Y., Kaixi H., and Panmao Z.: Shift in the temporal trend of boundary layer height in China using long-term (1979–2016) radiosonde data. Geophysical Research Letters, 46, 6080–6089. https://doi.org/10.1029/2019GL082666, 2019.

Heald, C. L., Jacob, D. J., Jones, D. B., Palmer, P. I., Logan, J. A., Streets, D. G., ... and Nehrkorn, T.: Comparative inverse analysis of satellite (MOPITT) and aircraft (TRACE-P) observations to estimate Asian sources of carbon monoxide. Journal of Geophysical Research: Atmospheres, 109(D23), 2004.

Kahn, R. A., A global perspective on wildfires, Eos, 101, https://doi.org/10.1029/2020EO138260, 2020.

Kahn, R. A., Chen, Y., Nelson, D. L., Leung, F. Y., Li, Q., Diner, D. J., and Logan, J. A..: Wildfire smoke injection heights: Two perspectives from space. Geophysical Research Letters, 35(4), 2008.

Kahn, R. A., Li, W. H., Moroney, C., Diner, D. J., Martonchik, J. V., and Fishbein, E.: Aerosol source plume physical characteristics from space-based multiangle imaging, J. Geophys. Res., 112, D11205, doi:10.1029/2006JD007647, 2007.

Kahn, R. A., A global perspective on wildfires, Eos, 101, https://doi.org/10.1029/2020EO138260, 2020.

Kauffman, J. B., Steele, M. D., Cummings D. L., and Jaramillo V. J.: Biomass dynamics associated with deforestation, fire, and, conversion to cattle pasture in a Mexican tropical dry forest, For. Ecol. Manage., 176, 1-12, doi: 10.1016/s0378-1127(02)00227-x, 2003.

Gunturu, U. B.: Aerosol-Cloud interactions: a new perspective in precipitation enhancement, 2010.

Paugam, R., Wooster, M., Freitas, S., and Val Martin, M.: A review of approaches to estimate wildfire plume injection height within large-scale atmospheric chemical transport models. Atmos. Chem. Phys., 16, 907–925, doi:10.5194/acp-16-907-2016, 2016.

Sofiev, M., Ermakova, T., and Vankevich, R.: Evaluation of the smoke-injection height from wild-land fires using remote-sensing data, Atmos. Chem. Phys., 12, 1995–2006, https://doi.org/10.5194/acp-12-1995-2012, 2012.

Val Martin, M., Kahn, R. A., Logan, J. A., Paugam, R., Wooster, M., and Ichoku, C.: Space-based observational constraints for 1- D fire smoke plume-rise models, J. Geophys. Res.-Atmos., 117, doi.:10.1029/2012JD018370, 2012.

Constraining the relationships between aerosol height, aerosol optical depth and total column trace gas measurements using remote sensing and models

Shuo Wang[1], Jason Blake Cohen[1, 2, *], Chuyong Lin[1], Weizhi Deng[1]

[1]School of Atmospheric Sciences, Sun Yat-Sen University, Guangzhou, 519000, China
[2]Southern Marine Science and Engineering Guangdong Laboratory (Zhuhai)

Correspondence to: Jason Blake Cohen (jasonbc@alum.mit.edu)

Abstract. Proper quantification of the aerosol vertical height is essential to constrain the atmospheric distribution and lifetime of aerosols, as well as their impact on the environment. We use globally distributed, daily averaged measurements of aerosol stereo heights of fire aerosols from MISR to understand the aerosol distribution. We also connect these results with a simple plume rise model and a new multi-linear regression model approach based on daily measurements of NO_2 from OMI and CO from MOPITT to understand and model the global aerosol vertical height profile over biomass burning regions. First, plumes associated with the local dry-burning season at mid to high latitudes frequently have a substantial fraction lofted into the free troposphere, and in some cases even the stratosphere. Second, plumes mainly associated with less polluted regions in developing countries and heavily forested areas tend to stay closer to the ground, although they are not always uniformly distributed throughout the boundary layer. Third, plumes associated with more serious loadings of pollution (such as in Africa, Southeast Asia and Northeast China) tend to have a substantial amount of smoke transported uniformly through the planetary boundary layer and up to around 3 km. Fourth, the regression model approach yields a better ability to reproduce the measured heights as compared to the plume rise model approach. This improvement is based on a removal of the negative bias observed from the plume model approach, as well as a better ability to work under more heavily polluted conditions. However, over many regions, both approaches fail, requiring deeper work to understand the physical, chemical, and dynamical reasons underlying the failure over these regions.

1 Introduction

Over the past few decades, there has been an increasing amount of research into the spatial and temporal distribution of atmospheric aerosols (Achtemeier et al., 2011; Cohen et al., 2017; Cohen et al., 2018). This has been in part because of the impacts that aerosols have on clouds, radiation, the atmospheric energy balance and climate, human health, and ecosystems, among other aspects (Cohen, 2014; Tao et al., 2013; Ramanathan et al. 2007; Ming Y. et al, 2010). However, there has not been a significant amount of research work done in terms of understanding the vertical distribution of aerosols in the atmosphere (Cohen et al., 2018), although such knowledge is essential to constrain their impacts the atmospheric energy budget (Kim et al., 2008; Grandey et al., 2018), circulation, clouds and precipitation(Cohen et al., 2011; Tosca et al., 2011; Singh et

Deleted: Val Martin et al., 2012; Nelson et al., 2013;

Deleted: Mims et al., 2010

al., 2018), and ultimate tropospheric distribution (Leung et al., 2007; Randles, et al., 2017). Large-scale reviews of the biomass burning literature spend a lot of time on how the atmosphere impacts the burning conditions, but also tend to overlook the issue of how the emissions are rapidly vertically distributed upon being emitted (Palacios-Orueta et al., 2005).

The vertical distribution of aerosols is observed to be more complex than the present generation of global and mesoscale models are capable of reproducing in regions where there are multiple sources with similar magnitudes and very different vertical lofting properties (Kahn et al., 2008; Petrenko et al., 2012; Chew et al., 2013). While on one hand urban sources are emitted with relatively low amounts of heat and are therefore known to remain in the boundary layer (Guo et al., 2016), on the other hand, biomass burning sources are emitted with large amounts of heat at high temperature and frequently are rapidly transported higher in the atmosphere, such that they are effectively emitted at height (Ichoku et al., 2008; Field et al., 2009; Freeborn et al., 2014). Furthermore, there are other forcing mechanisms, such as deep convection (Petersen and Rutledge 2001; Turquety et al., 2007), volcanos (Singh et al., 2018; Flower and Kahn, 2017), mountain slope winds (Cohen et al., 2017), and other dynamical forcings (Cohen et al., 2011; Tosca et al., 2011) which also have a substantial effect on the vertical distribution of aerosols over specific spatial and temporal scales. The vertical distribution of aerosols has a direct impact on their lifetime and hence atmospheric loading, with aerosols lofted above the boundary layer having a significantly larger impact the atmosphere than those emitted into the boundary layer (Nelson et al., 2013; Paugam et al., 2016). Therefore, understanding the vertical distribution over the source regions (Nelson et al., 2013) of aerosols and how this may change over time is absolutely critical for our being able to better constrain the environmental and atmospheric impacts.

Currently, aerosol data comes from different measurements made from the surface, balloons, aircraft, and satellites, with varying degrees of accuracy (Husar et al., 1997, Jost et al., 2004, Rogers et al., 2011) used in-situ measurements to observe the plume from North American fires emitted at a surface temperature above 380K, and found that carbon monoxide and tiny particles were detected in the stratosphere at an altitude of 15.8 km. Kahn et al. (2007) found using MISR measurements that 5% to 18% of smoke plumes reached the free troposphere over Alaska and the Yukon Territories in 2004. Winker et al. 2013 introduced the idea of possibly using CALIPSO lidar as a measurement technique, since it is more sensitive to dispersed vertical aerosols away from fire points than MISR satellites, and therefore could capture the overall smoke cloud better. Val Martin et al. (2018) used MISR data with pixel-weighted and AOD-weighted statistics to estimate the impact of fire severity of on fire height and found that while in the Arctic there were significant areas with aerosols found above the boundary layer, in agricultural areas and most other non-arctic areas, the amount was small or non-existent. Cohen et al. (2018) produced the first comprehensive study using CALIPSO lidar data anywhere in the world, and found that throughout the 2006 biomass burning season in Southeast Asia that 51% to 91% of smoke from fires was ultimately found to reside in the free troposphere. This is consistent with earlier theory by which show that when a plume is injected into the free troposphere, it tends to accumulate in a relatively stable layer (Val Martin et al., 2010; Kahn et al., 2007).

Deleted: Winker et al., 2013)

Deleted: 7

Deleted: Vernon et al., 2018

Deleted: Val Martin et al. (2018)

Deleted: in almost

Deleted: all areas, there is a large amount of aerosols above 2 km

The present generation of models have not been found to reproduce the vertical distribution of aerosols very well (Val Martin et al., 2012; Paugam 2016; Cohen et al., 2018). Most of the previous approaches to simulate convection induced by a fire or other surface heat sources have been performed with simplified models (Briggs, 1965; Trentmann et al., 2006). There have been multiple studies using global and regional chemical transport models (CTMs) with such simple plume models built in to try to understand the impact of fire emissions on air quality and atmospheric composition (Pfister et al., 2008; Turquety et al., 2007; Spracklen et al., 2009; Ichoku and Ellison 2014). There have also been other attempts to simulate the impacts of different vertical distributions based on higher-resolution wind patterns profiles, done on a region-by-region basis (Cohen and Prinn, 2011; Cohen and Wang, 2014). More recently, people have attempted to use Lagrangian models such as Dewitt and Gasore (2019) and Vernon et al. (2018), to understand how knowledge of air mass flows could better contribute to the understanding of different vertical regions having material from biomass burning plumes found far upwind. Val Martin et al. (2012) used a 1-D plume rise model to study plume heights over North America, which demonstrated dynamical heat flux and atmospheric stability structure affect plume rise. Cohen et al. (2018) also adapted a plume rise model and found that significant enhancements were required to the measured Fire Radiative Power (FRP) values in order to match the mean values of measured heights, although the upper and lower quartiles were not able to be successfully reproduced. At present, there is no known modelling work that can accurately and consistently reproduce this substantial atmospheric loading found throughout different regions of the world in the upper boundary layer and free troposphere.

Biomass combustion is a major source of trace gases and aerosols in the atmosphere as well as having an important impact on tropospheric ozone formation. The vast majority of biomass burning in the tropics and non-tropical agricultural regions of the world is a man-made activity (Kauffman et al., 2003; Achtemeier et al., 2011; Paugam et al., 2016), while in certain arctic regions, lighting accounts for a significant amount of biomass burning (Generoso et al., 2007). In particular, this activity has been shown to have a strong annual cycle (Cohen et al., 2017; Labonne et al., 2007; Tsigaridis et al., 2014). The process of burning releases heat, increasing the local temperature of the surrounding air, resulting in a change in buoyancy and an ensuing updraft above the heat-producing area. Based on how long the plume maintains its buoyancy, it will rise to a fairly high position in the atmosphere. However, strong turbulence causes the plume to mix with the surrounding air, reducing plume temperature and buoyancy, eventually reaching a stable layer at which the updraft stops (Damoah et al., 2006; Freitas et al., 2007). For these reasons, a significant amount of the material emitted from biomass combustion is lofted above the surface, as compared with urban sources, where almost all of the aerosol remains near the surface (Ichoku et al., 2008; Cohen and Prinn 2011). This point is important because if aerosol is injected into the atmosphere above the planetary boundary layer (PBL) they can be carried by the faster free tropospheric winds farther away, leading to a larger impact on the atmosphere (Vernon et al., 2018; Nelson et al., 2013).

The present generation of models has difficulty to reproduce the actual vertical distribution of atmospheric aerosols when addressing cases that do not tend to have a combination of a highly energetic fire source, a relatively dry atmosphere, and a

Deleted: Ichoku and Ellison, 2014

relatively optically thin smoke column emitted by the fire. One reason stems from the fact that in-situ production and removal mechanisms of aerosols as well as the distribution of rainfall are not fully understood (Tao et al., 2012), all of which weaken the ability of simple plume rise models to reproduce the vertical distribution of aerosols (Urbanski 2014; Cohen et al., 2017). In addition, heterogeneous aerosol processing associated with the highly polluted conditions within the atmospheric plume may also change the hygroscopicity, which in turn impacts the washout rate and vertical distribution of the aerosols (Kim et al., 2008; Cohen et al., 2011). On top of this, highly polluted aerosol loadings, especially so for absorbing aerosols as found in fires, lead to changes in the radiative equations and the vertical atmospheric stability (Guo et al., 2019; Cohen et al., 2018; Zhu et al., 2018). Furthermore, small scale convective events and large-scale circulation patterns are generally not both well produced by the same scale models, leading to an inherent bias against one or the other convection producing source (Winker et al., 2013; Jost et al., 2004). In summary these factors can lead to actual changes in the vertical distribution of aerosols that simple models are not able to reproduce, including those which have used inverse modeling with a fixed vertical a priori (i.e. Heald et al. 2004; Cohen and Prinn, 2011), in turn affecting the distribution of aerosols hundreds to thousands of kilometers downwind, supporting new measurement-based perspectives (i.e. Kahn 2020).

This work describes a new approach to comprehensively understand global-scale, daily measurements of the vertical distribution of aerosols, and introduces a simple modeling approach better capable of reproducing the vertical distribution of smoke aerosols emitted by biomass burning. First, we analyze the plume heights from three and a half years of daily Multi-angle Imaging SpectroRadiometer (MISR) satellite measurements, separating the more than 67,000 measurements by the magnitude of the measured variability. Next we build aerosol plume injection models depending on the region, terrain, land type, and geospatial properties. We use this simple plume model to show that the aerosol injection heights are underestimated. We then apply a linear statistical model and show that including measurements of column gas loadings from other satellites in combination with the meteorological and FRP measurements produces a better match. We imply that ignoring the magnitude of the source emissions is an important factor in the plume rise height, another factor which the current generation of models does not take into consideration. We also demonstrate that improvements in the local convective transport process and direct and semi-direct effects of aerosols are needed to further reduce the error between the models and measurements.

It is hoped that these results will provide insights to further improve our understanding of the vertical distribution of aerosols, both from the modeling side, and from what sources of information are best required from the measurement community to help the modelers improve their understanding. We also provide a unique perspective on the connections between air quality and the vertical distribution of particulate matter, allowing the community make further advances in these fields as well as associated issues of long-range transport of aerosols as well.

2 Methodology

2.1 MISR Aerosol Height Measurements

MISR, the Multi-angle Imaging SpectroRadiometer, is an instrument flying on the Terra satellite capable of recording images at 9 different angles over 4 bands at 446nm, 558nm, 672nm, and 866 nm. The cameras point forward, downward, and aftward, allowing images to be acquired with nominal view angles, relative to the surface of 0, ±26.1, ±45.6, ±60.0, and ±70.5 degrees. All cameras have a track width of 360 km and observations extending within ±81 degrees latitude (Kahn et al., 2007). In this paper, we use the MISR INteractive eXplorer (MINX) software, which captures the plume height from the MISR image and combines it with the MODIS fire point measurements (also taken on the Terra satellite). The software then calculates the wind speed and the elevation of contrast elements globally over a 1.1 km pixel area, providing a digitization of wildfire smoke plume height (Val Martin et al., 2010; Kahn et al., 2007; Nelson et al., 2013).

2.2 Geography

Around the world, biomass burning and deforestation have undergone tremendous changes in the past few decades, with current extremes making the news in many places throughout the world. To better interpret the land use conditions in the biomass burning areas, we apply global land-cover type data of 18 different vegetation types, as measured in 2015 in Fig. 1. This work specifically focuses on those areas where the land type has undergone known significant changes from forest to agriculture, or from forest or agriculture to urban, as demonstrated in the black boxes in Fig. 1.

Deleted: We

Considering MISR daily plume heights (where the 1.1km pixels are first averaged to 10km x 10km grids) throughout the globe, we have determined that the respective average and standard deviation of the plume height over the three and a half years of MISR daily measurements (from January 1 2008 through June 30 2011) are 1.37km and 0.72km. However, over our regions of interest, we find that we are able to capture the large bulk of the standard deviation globally, as demonstrated in Table S1.

The geographical data yields us a few conclusions about those regions which have the largest contribution to the biomass burning height variation. First, they are distributed in the middle and low latitudes (between the Tropic of Cancer and the Tropic of Capricorn) and/or high latitudes (near the Arctic Circle). Second, they tend to occur in regions of more rapid economic growth, and/or in regions which are experiencing the most rapid change in land surface temperature.

2.3 MOPITT Carbon Monoxide (CO) Measurements

Carbon monoxide (CO) is a colorless and odorless gas that plays a major role in moderating the chemistry of the Earth's atmosphere as well as having a deleterious effect on human health. One of the world's major sources of CO is emissions from biomass burning. For these reasons, we obtain measurements of CO from the MOPITT satellite (an instrument mounted on

NASA's Terra satellite), which has collected data since March 2000. MOPITT's resolution is 22 km at nadir and observes the Earth in swaths that are 640 km wide.

In terms of the CO from MOPITT, we take the day time only retrievals (to reduce bias) from version 8, level 3 data, from January 1, 2008 through June 30, 2011. In specific we use the combined thermal and near infrared product (Deeter et al, 2017). We further constrain the data to where the cloud fraction is less than 0.3 and where the vertical degrees of freedom are larger than 1.5. This combination has been shown to allow us to trust that there is a sufficient amount of signal and knowledge to demonstrate an actual measurement in the vertical, as compared with a result only dependent on the a priori model, as shown in Lin et al. (2020a). There are further gaps in the data due to orbital locations and very high aerosol conditions, all of which prevent entire coverage of our areas of interest each day. Therefore, we average all of the individual MOPITT data that passes our test to a 1°x1° grid.

2.4 OMI Nitrogen dioxide (NO_2) Measurements

Another chemical species co-emitted by biomass burning with aerosols and CO is NO_2 (Seinfeld and Pandis, 2006). For this reason, we also use the daily average total column loading of NO_2 as measured by the Ozone Monitoring Instrument (OMI). In specific we use version 3 Level 2 measurements taken from the Aura satellite (Boersma et al., 2007; Lamsal et al., 2011; Levelt et al., 2006), which has ground pixel sizes ranging from 13kmx24km at nadir to about 13kmx150km at the outermost part of the swath. In terms of the NO_2 from OMI, we first take the daily retrievals under the conditions where the cloud fraction is less than 0.3. Next, we aggregate the data to 0.25° x 0.25° using a linear interpolation and area weighted approach. In this way, those measurements near the edge of the swath or which are adjacent to cloudy areas are weighted less heavily in terms of the merged product. However, the areas are sufficiently large as to be roughly representative of the emissions from biomass burning of the NO_2 from within the grid box, as compared to that transferred from adjacent grid boxes.

One advantage of the OMI NO_2 column measurements is that they can often be observed under relatively cloudy or smoky conditions (Lin et al., 2014). Another advantage is that the atmospheric lifetime of NO_2 is only a few hours, and therefore relatively large changes in the temporal-spatial distribution of NO_2 column measurements is highly correlated with wildfire sources (Lin et al. 2020a). NO_2 has another interesting property in that its production/emissions is a strong function of the temperature at which the fires are burning, since NO_2 is formed based on the air temperature (Seinfeld and Pandis, 2006).

2.5 Plume Rise Model

Although emissions from biomass burning are similar to those from urban combustion sources, there are two major differences, arising from the much higher burning temperature and the environment in which the combustion occurred. This ensures that a significant amount of the emissions from biomass burning will be transported upwards due to the positive

Deleted: with the

Deleted: being

buoyancy generated by the fire. Due to the confluence of both local and non-local dynamical forcing in-situ, the ultimate height reached by these emissions is a complex function of the local fire energy and both the local and large-scale meteorology at the time of combustion. While the aerosol particles are immediately transported horizontally by the large-scale winds, their vertical rise will only stop once their local buoyancy has reached equilibrium, and any dynamical motion has degraded back to the background conditions (Freitas et al., 2007; Sofiev et al., 2012; Val Martin et al., 2018).

To approximate this rise, we use a simple plume rise model (Briggs, 1965) to generate the final injection height of the biomass burning emissions based on the buoyancy and horizontal velocity of the plume and various atmospheric conditions. Although this model is based on an empirical formula mathematically, it is essentially a thermodynamic approximation (Cohen et al., 2018) which costs much less computationally as well as being quite efficient when the biomass burning source covers a large area.

In theory, if such an approach was successful, and it was given appropriate environmental data, it should be able to reproduce the heights derived from the MISR multi-angle measurements. For this reason, we use a 1-D plume rise model to independently predict the position and height of each measured MISR plume at each 10km x10km grid which is found to have measurements. To initialize the model, we require meteorological data as well as MODIS hot-spot information.

2.6 NCEP Reanalysis Data

NCEP and NCAR produce an analysis/prediction system to produce a meteorological field analysis of the 6-hourly state of the atmosphere from 1948 to the present. The measurements incorporated into this approach include ground based, in-situ, and remotely sensed sources, while the modeling aspect is based on state-of-the-art meteorological models. Daily data for each day which has MISR data is obtained from the reanalysis version 1 (Kalnay et al., 1996). Only data required to run the plume rise model is used: the vertical temperature and pressure distributions, the surface air temperature, and the initial vertical velocity of the smoke emissions (dP/dt). The vertical temperature gradient (dT/dz) and the vertical velocity (dz/dt) are computed from this data.

Deleted: In specific, we obtain d

Deleted: which we have

Deleted: Specifically we use the data

Deleted: for us

Deleted: We then compute the

2.7 Regression Model

Linear regression is a simple method by which one can relate the impact that a set of orthogonal inputs have in terms or reproducing measured environmental values. It does not imply causation, merely demonstrating that the input values behave in a similar manner. However, when looking to describe whether or not a new variable has a substantial amount of correlation with a given phenomenon, it can be found to be very useful.

In this case, we are interested to see if the loadings of NO_2 and CO are related to the heights of the fires. There is a strong physical case to be made here, since both are directly emitted by the fires themselves. Furthermore, the underlying causes of

these substances are different: NO_2 is a function of the fire temperature, while CO is a function of the Oxygen availability. Furthermore, these are proxies for radiatively active substances such as soot and ozone.

For our work, we have decided to apply a simple linear regression model of the wind speed, FRP, CO, NO_2, and the ratio of NO_2/CO. FRP is the measure of the radiative energy released by the fire. It is usually found in the infrared part of the spectrum as this is the part of the EM spectrum that corresponds closely with the temperatures that fires occur at in the Earth System. This is because the traditional plume rise models always include wind speed and FRP in their representations, so we wanted to specifically include as many different representations of the co-emitted gasses as well, as given in Equations 1-7.

$$H_1 = \alpha * V_{wind} + \beta * W_{FRP} + \gamma * [CO] + \delta * [NO_2] + C \ , \quad (1)$$

$$H_2 = \alpha * V_{wind} + \beta * W_{FRP} + \gamma * [CO] + \varepsilon * ([NO_2]/[CO]) + C \ , \quad (2)$$

$$H_3 = \alpha * V_{wind} + \beta * W_{FRP} + +\delta * [NO_2] + \varepsilon * ([NO_2]/[CO]) + C \ , \quad (3)$$

$$H_4 = \alpha * V_{wind} + \beta * W_{FRP} + \gamma * [NO_2] + s \ , \quad (4)$$

$$H_5 = \alpha * V_{wind} + \beta * W_{FRP} + \gamma * [CO] + C \ , \quad (5)$$

$$H_6 = \alpha * V_{wind} + \beta * W_{FRP} + +\varepsilon * ([NO_2]/[CO]) + C \ , \quad (6)$$

$$H_7 = \alpha * V_{wind} + \beta * W_{FRP} + C \ , \quad (7)$$

We calculate all of the correlation coefficients (R^2>0.2) between the different models and the MISR measurements, ensuring that (P<0.05). Finally, we analyze both the magnitude of the regression coefficient as well as the magnitude of the various best-fit terms. These models are then used to reproduce the aerosol heights and are ultimately compared with both the plume model and the actual measurements.

The seven different regression models were chosen so as to cover the entire combination of different ways to fairly and uniformly incorporate the CO and NO_2 measurements as well as their underlying physical meanings. The 7th regression model is the approximation of the plume rise model. The 4th and 5th regression models are the approximations of the single-species linear impact of NO_2 and CO respectively. The 6th regression model approximates the single-species non-linear impact of NO_2 and CO in tandem. Finally, the 1st through 3rd regression model are the approximations of the combination of CO and NO_2 in tandem with both linear (model 1), or with one linear and one non-linear combination (models 2 and 3). This approach is consistent with and follows from some of the earlier works which tries to use advanced learning to understand some higher order, simple non-linear forcings, still based on some physical consideration, i.e. Cohen and Prinn, 2011.

2.8 MERRA

To obtain another independent dataset of aerosol height over the biomass burning regions, we use the NASA MERRA-2 hydrophobic black carbon product (Randles, et al., 2017). MERRA is a reanalysis product based on the GEOS-5 GCM and

meteorology suite with an output resolution of 0.5° x 0.625° every 3 hours. The underlying aerosol model is based on GOCART aerosol, which assumes independent, non-mixed aerosols, and hence is not an ideal environment for the high concentrations and intense mixing that occurs over biomass burning regions (Petrenko et al., 2012). The assimilated aerosol fields are mostly from MODIS and AVHRR, with a small amount of input from MISR over bright surfaces and AERONET where it exists. There are however known issues with respect to MERRA and biomass burning (i.e. Buchard et al., 2015). For these reasons, we average the 8 3-hour time periods together for each respective day of interest, and use the information from 500mb to the surface.

3 Discussion and Results

We approach this problem with additional measurements compared to what are normally made so that we can have a deeper insight into how these somewhat related species have on height to which aerosols from biomass burning rise in the atmosphere. Due to the fact that there are additional processes in-situ which can lead to heating, cooling, and other changes to the dynamics, it is essential that we establish any first-effect relationships, and then work more deeply as a community to address them in turn.

First, we to enforce consistency, we impose a condition that for all days analyzed, we must have data present from all of the data sources: MISR, MODIS, MOPITT and OMI. On this basis, we explore the relationships between the two basic data sets (MISR and MODIS) and the source regions. By choosing regression models that both represent the format of the plume rise model as well as those that do not, but are instead based on additional information from MOPITT and OMI, we are thereby including this data in a way that is consistent with the underlying science and without bias.

Second, since these datasets make measurements with different assumptions, we also will reduce our bias in our inputs measurements as a function of clouds, different burning conditions, radiation feedbacks, and other actual atmospheric effects. We hope that this will help us to more clearly clarify the actual atmospheric phenomena responsible for the vertical transport, which a more conventional plume rise model may not be able to account for.

Third, the range of the seven regression models is an attempt to intelligently account for the fact that the column loadings of the CO and NO_2 offer physical meaning and insight, as compared to merely being an attempt to minimize any unexplained variance. We argue that the column values of both CO and NO_2 are both directly and indirectly related to the magnitude and the height of the vertical aerosol column. Due to the fact that the emissions of NO_2 is a strong function of the fire temperature, and its short atmospheric lifetime, the NO_2 is strongly related to the temperature of the fire, or the FRP, which is one of the essential driving forces of the buoyancy. This issue is strongly coupled with the fact that FRP is also one of the most error-prone of the measurements commonly used to drive the plume-rise models, with the FRP commonly underestimated in the tropics due to clouds and aerosols, as given in Kaiser et al. (2012), Cohen et al. (2018), and Lin et al. (2020a). Additionally,

the amount of CO produced is a function of the total amount of biomass burned as well as the wetness of the surface itself where the burning occurred, and hence the CO column loading is also physically related to the properties of the fires. In fact, using a measure of the CO column can help us to overcome the physical constraints that current measurements have in terms of addressing the issues of how much peat or understory has burned, or if such fires which are occurring without direct line of sight from above can even be detected by the current fire detection processes at all (Leung et al., 2007; Ichoku et al., 2008). The combination of high NO_2 (which is more produced at higher temperature) and low CO (which is more produced at higher temperature) means that the ratio of NO_2 to CO also provides further physical insight into the non-linearities associated with the fire temperature, wetness, and possibility of other heat sources/sinks at the fire/atmosphere interface such as smoldering, conversion to latent heat, etc.

3.1 Characteristics of MISR, OMI and MOPITT species

We use a PDF analysis to look at the distribution of the daily fire-constrained aggregated Measurements from MISR from each region over the entire dataset from 2008 to 2011 in Fig. 2. The statistical mean and standard deviation over each region are given in Table S1. We determine that the height of measurements ranges from 0 to 29 km (with extremely high values in the middle stratosphere possibly an error), which is not only higher than previous studies (Cohen et al., 2018; Val Martin et al., 2018), but also includes some extreme events which have made their way into the stratosphere. Due to the fact that first, the majority of the plumes are injected into the boundary layer or the lower free troposphere, second that this paper is not looking into the underlying physics of stratospheric injection (Pengfei Yu et al., 2019), and third that plumes tend to accumulate within layers of relative atmospheric stability, therefore an upper bound cutoff on the measured values of 5000m is imposed. This is consistent with the fact that over the regions of interest in this work, fewer than 0.48% of the total plume heights are more than 5 km.

There are very different distributions of the measured heights over the different regions Fig. 2. The corresponding mean, standard deviation, and skewness of the heights over each respective region is given in Table S1. The average percentage of the data which has a measured height above 2 km (selected because it is always in the free troposphere) is 15.0%, with the lowest in Central Canada of 41.7% and the highest in Midwest Africa of 0.8%. In terms of the amount of data measured with a height more than 4km, the average over the globe is 1.5%, while the range is as high as 6.6% in Central Canada and as low as 0.1% in Midwest Africa and Northern Australia. On the other end of the comparison, some regions which are very polluted near the surface, while others show the vast majority of their heights are elevated off the ground. To safely consider those plumes which are definitively near the surface (i.e. never above the boundary layer) a plume height below 200m would roughly corresponds to the boundary layer maximum in the middle of the day (Guo et al., 2019). However, due to the measurement uncertainty of the MISR heights being between 250m and 500m, instead the percentage of total plumes with a height below 500m is chosen, which is found to have a total percentage of respective plume heights of: global (1.1%) and a range from a

Deleted: we
Deleted: are
Deleted: we
Deleted: want to set
Deleted: that we will not consider after this point
Deleted: Given the fact that the total percent of measurements over 5000m is less
Deleted: 7
Deleted: 9
Deleted: , we therefore only look at data with an upper limit of …
Deleted: for the remainder of this work
Deleted: We first observe that t
Deleted: we also have
Deleted: Overall, we have a
Deleted: 2
Deleted: (the minimum rough level of the boundary layer through the day) with a
Deleted: mean of 2
Deleted: .3
Deleted: ,

minimum of 0.68% in Southern Africa to 49% in Argentina. Given the diversity of these results, there is a need to more deeply understand the driving factors across all of these different regions, as well as the importance of biomass burning in terms of transporting aerosols through the boundary layer.

Second, we perform a comparison across the different daily time series of measured aerosol heights, CO column, and NO_2 column as aggregated from January 1, 2008 to June 30, 2011 over all of the biomass burning regions Fig. S1. We consider the burning season to be when we observe aerosol plumes and a peak in at least one of the CO and/or NO_2 column measurements. Furthermore, MISR has a relatively narrow swath, not providing daily coverage to all points, coupled with a morning overpass time which may lead to negative bias in some regions and positive bias in other regions in terms of observed fires. This combination allows us to clearly demonstrate that the observed smoke peaks are in fact due to burning of a significant amount of material, and are true cases of biomass burning, while not possibly being fully representative of all biomass burning events. In the observed cases, the peak occurs from November to March in Central Africa, Midwest Africa; June to September in Central Canada, Eastern Europe, South America; April to July in Central Siberia; May to December in Southern Africa, Northern Australia; January to April in Northern Southeast Asia; March to September in Siberia and North China; April to September in West Siberia. In addition, the length of the peak burning time is also an important consideration which varies greatly across the different regions. The length of the total number of burning days from the three and a half years of data is an average is 108 days, with a minimum of 14 days in Eastern Siberia and a maximum of 388 days in Southern Africa.

Next, we look at the impact of FRP measurements and buoyancy in terms of the plume height distribution. In general, the higher the FRP, the higher the plumes should rise. However, these measurements seem to include a larger number of total measurements into the lower free troposphere than previous plume rise model studies have been able to account for. From our measurements, we notice that the FRP (as computed on average over 1.1kmx1.1km grids where a fire exists) has a global mean of 37.7W/m^2 and a reginal minimum and maximum of 31.1W/m^2 (Siberia and North China) and 82.6W/m^2 (Central Canada) during the respective biomass burning seasons. Analyzing the extremes of the FRP, leads to a top 5% of measured FRP of 132W/m^2 and a bottom 5% of measured FRP of 8.5W/m^2.

Based on previous work, we would expect a general plume rise model to not be able to match the observed heights well under these conditions, since the observed FRP is too low (Cohen et al., 2018; Gonzalez-Alonso et al., 2019). The high end of the FRP range of the observations in this work is not considered to be very hot in terms of fires, which should in theory help to reduce the known plume rise model bias of underpredicting very strong FRP conditions, leading to an overall improvement in the plume rise model as analyzed in this work, as compared to when it is less constrained. As expected, there are more plumes found above the boundary layer in the measurements corresponding to very high FRP values than in the case of very low FRP values, although more importantly, there still are plumes found over the boundary layer in both cases, which is not expected based solely on the plume rise model formulation. One possible explanation for this phenomenon is that the biomass

Deleted: 04
Deleted: Central
Deleted: 6.7
Deleted: at Western Siberia
Deleted: se
Deleted: we
Deleted: is
Deleted: se

burning occurring during the times of year where there is a negligible impact on the atmospheric loadings of NO_2 and/or CO is significantly more energetic and therefore has a very different height profile, as compared to the times when the most emissions of NO_2 and/or CO are produced. Another explanation is that there is additional forcing which are also playing a role in terms of the aerosol plume height rise that are independent of the FRP. Yet another possibility (Mims et al., 2010; Val Martin et al., 2018) is related to there being some type of problem with the presentation of the nature of the land-surface itself, since fires occurring in heavily forested and agricultural areas are likely to have significantly different vertical distributions. On top of this, there may be partially filled pixels in the remotely sensed measurements (Kahn et al., 2007; Val Martin et al. 2012). Finally, it is possible that the intense aerosol loadings themselves are leading to absorption of a significant amount of the IR radiation which is in turn biasing the FRP measurements too low (Cohen et al., 2017; Cohen et al., 2018).

It is also possible that there are significant differences to be found in the non-linearity between FRP and the wind speed. Interestingly, if the horizontal wind speed is quite high when the air passes over the fire source, it will cause turbulence and vortices, resulting in a lifting force. On the other hand, if the wind speed is too high, it will bend the plume's momentum and reduce the upward transference based on any initial vertical injection velocity. Furthermore, the wind speed may have different relationships with convection, which itself plays a dominant role in the rise of the plume. Given these effects, we do not directly consider wind-speed and the plume rise height independently, only within the confines of the plume rise model.

Since there are many underlying direct and indirect theoretical physical and chemical connections between the loadings of the CO and NO_2 and the overall plume heights from MISR, we want to investigate this possibility more deeply. To make this comparison, we first looked at the entire time series, not only those periods during which the measured aerosol heights obviously had an impact on the atmospheric loadings of the CO and NO_2. Next, we selected days which had data from all three measurement sources: MISR, MOPITT, and OMI. Furthermore, since we could not find such a paper in the literature, we have decided to keep the relationship open and simple, without worry of over-constraining any relationship found. In theory, the injection height of the aerosol plume is related to the emission of smoke in the wildfires, since this is a function of the amount of heat released. Therefore, we would expect that higher emissions of CO and NO_2 should correspond to higher heights of aerosols. However, the formation mechanisms of these two trace gasses is different, with CO a function of oxygen availability (and possibly surface wetness), while NO_2 is a function of the temperature of the burning. Furthermore, very high co-emitted levels of aerosols with the very high levels of trace gasses could also lead to a change in the vertical profile of the heating (Freitas et al., 2007).

To ensure that the variables are relatively independent, our analysis only considers only three mixtures of these species: the independent concentrations of CO, NO_2, and the ratio of NO_2/CO. We then investigate how changes in the loadings of NO_2, CO, and the ratio of NO_2/CO are associated with changes in the height of the plume. Furthermore, we need to consider the more extreme conditions in addition to the means, and are particularly interested in seeing how well loadings of the CO and NO_2 can be used to model those conditions where the plume heights are extreme.

Deleted: multiple

Deleted: the two with each other

Deleted:

Deleted: and/or

In all of the regions of the world, with the exception of the case of NO_2 over Siberia and Northern China, we have a case where the mean value of the CO and NO_2 measurements is higher over the set of points where the actual FRP measurements were made, than over the region as a whole Table 1. This is the point of this work, since we want to focus on the measured values from MOPITT and OMI which correspond to the same spatial locations as the measured FRP. This makes sense, since the magnitude of emissions from fires is very large compared with the non-burning season and/or surrounding areas. However, the differences in the CO are in generally smaller than for NO_2, which is further consistent with the fact that the lifetime of CO is much longer than that of NO_2. Thankfully the case is well understood over Siberia and North China is because there are some known significant urban areas nearby to the burning regions. Furthermore, this exception occurs in winter, where we know there is a significant enhancement of NO_2 emissions due to the increase in urban biomass burning to offset the brutally cold winter conditions.

Over these fire-constrained points, we find that the variability of both CO and NO_2 remains very low when computed on a point-by-point basis. On the other hand, over the entire regions, the variability of the point-by-point measurements of both NO_2 and CO are much higher. This is in large part due to the rapid changes in different land-use types in different parts of the regions of interest being studied (consistent with Cohen et al., 2018). These results are based on the statistics of more than 67000 daily MISR measurements. Therefore, for the remainder of the work, we only use the data for the NO_2 and CO which are obtained at points where FRP measurements exist.

Note that the measurements and the results here are looking at the aerosol heights measured over small spatial and temporal domains. We are looking to analyze the impact of the initial plume rise, and any very rapid adjustments in the atmosphere. The plume heights, both measured and modeled are not consistent with large-scale transport due to meteorology, factors enhancing the stability of a layer or changing the chemistry within a plume. They certainly are not receptive to a Lagrangian type of modeling effort, which is supposed to be focused on the air itself and in particular air at the large scale. Therefore, the results given here show here are the best methods currently used to reproduce the spatial distribution of aerosol plumes produced by wildfires.

3.2 Plume Rise Model Applied to MISR and Meteorological Measurements

The annual average global total cumulative FRP from 2008 to 2011 is 209 MW, based on more than 16000 measured MODIS fire hotspots. Overall, the measured FRP has been shown to be on the rise in recent years (Cohen 2018; Freeborn et al., 2014), although there is still a fundamental and significant amount of underestimation based on the current measurement techniques (Giglio et al., 2006). The plume rise model in theory should take these FRP values, and combine them with knowledge of the vertical thermal stability and the wind speed, to approximate the height to which the plume ultimately rises at equilibrium with its environment.

However, in reality, direct and semi-direct effects are not considered when using the simple plume rise model, although they are known to be important (Tao et al., 2012). Therefore, a different approach which attempts to take these forcings and/or the underlying aerosol loadings into account may lead to a better representation of the plume height rise, if such a model can be parameterized. Furthermore, the plume rise model relies on the atmospheric stability, and therefore does not take into account rainfall, changes in fire burning, in-situ chemical and physical production and removal, as well as the afore mentioned interactions radiatively between the aerosol and the atmospheric environment. This finding is consistent with evidence that the vertical plume rise and distribution of tropical convective clouds is sometimes dominated by in-situ heating and turbulence even more so than the initial heat of condensation (Gunturu, 2010).

All of these shortcomings aside, the use of simple plume models is the current scientific standard approach, and therefore we will apply it here as well. This is done by first aggregating the daily statistics of the vertical aerosol height over all parts of each region of interest Table 2. Direct comparisons are made between the modelled heights and the measured heights, and we find that 5 of the 14 regions studies in this work were shown to have a good match: West Siberia; Alaska; Central Canada; Argentina; Eastern Europe, where the modelled (and measured average heights) respective are 0.79 km (0.95 km) 1.39 km (3.03 km), 1.73 km (2.19 km), 0.65 km (0.25 km), 1.27 km (2.67 km).

Next, we look at the difference from day-to-day at each of the sites which has a mean value less than or equal to 0.25 km. Using these results, we find that the mean daily difference between the plume rise model and the MISR measurements as a whole show a large amount of variation, with a global average of 0.44 km, a maximum of 1.13 km (in West Siberia), and a minimum of 0.04 km (in Argentina). Across all of the different regions we find that the plume rise model underestimates the plume height. Furthermore, we find that the differences between the plume rise model and MISR are not normally distributed, with higher values not being able to be reproduced under any conditions, strongly indicative of a bias, in that somehow the largest, hottest, or most radiatively active fires are those being not reproduced well by the plume rise model. In addition to this, we compute the RMS error (Table 3) as a way of quantifying overall how well the model and MISR match. The RMS is found to be considerably larger than the difference of the means, indicating that a small number of extreme values are dominating the overall results, which were found to be 0.67 km, 0.88 km, 1.36 km, 0.40 km, and 0.85 km in the respective five areas.

To more carefully determine the extent of any bias, we analyze the PDF of the model and measurement results Fig. S2. This approach yields a clear determination that the plume rise model consistently underestimates the measured injection height, with the underestimate ranging from 6% (in Argentina) to 66% (in Southern Africa), and a global average of 33%. However, if we constrain ourselves to those fires occurring only in heavily forested regions, the average underestimate is reduced considerably to 11%. On the other hand, if we look across Africa as a whole, we find that the underestimate is on average 52%, a finding which deviates more from the measured aerosol vertical distribution than previous global studies (Val Martin et al., 2018) as well as those over Southeast Asia (which previously has been considered one of the world's worst performing

regions for such plume rise models, such as Reid et al., 2013; Cohen, 2018). The only region over which the finding may not be statistically relevant is in Alaska, where the difference between regression measurements are all constrained to within a 500m height band, which falls into the MISR measurement uncertainty measurement range.

Furthermore, even though the plume rise model leads to a low bias compared with the measured height, it is still not ideal for very low plumes which are found near the surface. The plume rise model tends to instead uniformly overestimate the amount of aerosol found in the upper parts of the boundary layer from 0.5km to 1.5km, while at the same time not providing any reliable amount of prediction for the cases where there is a considerable amount of aerosol under 0.5km. For example, the plume rise model is sometimes a good fit for aerosol heights under 0.5 km such as in West Siberia and Eastern Europe (where 23.5% and 12.3% of the measurements are under 0.5km and 27% and 13.6% of the plume rise model heights are under 0.5km, respectively). However, in other locations, the plume rise model grossly overestimates the amount under 0.5km such as in Central Africa and East Siberia (where 3.6% and 17.9% of the measurements are under 0.5km and 20.5% and 51.0% of the plume rise model heights are under 0.5km, respectively). In the case of Argentina there is a slight underestimate of the 0.5km heights by the plume rise model (49.4% of measurements and 30.1% of the plume rise model heights). One of the reasons for this is that in general the plume rise model tends to underestimate the results from 1.5km to 2.5km, and cannot reproduce results reliably at all above 2.5km. This is partly due to the effect that the FRP values are too low, and possibly due to other processes occurring in-situ which further lead to buoyancy and/or convection.

A few special regions of interest have been observed when comparing the plume rise results with the measurements. In Southern Africa plumes cover 9763-pixels or 19% of the total research area, and therefore are extremely representative of the overall atmospheric conditions. What is observed is that there is almost no aerosol (only 5.9%) present close to the ground (from 0km to 1km). The vast majority of the aerosols, 92.6%, are concentrated from 1km to 3km. Furthermore, we observe that the time series of both CO and NO_2 loading is significantly higher than other regions Fig. S1. This finding is completely the opposite form the plume rise model result, which shows that most of the pollutants (97%) are concentrated in the range of 0-1km, while almost none (3%) is found from 1km to 3km. There are a few reasons for this finding. First of all, when both CO and NO_2 loadings are high, the aerosol concentration and AOD will also be high, since they are co-emitted at roughly similar ratios from the fires. This in turn will both lead to a further underestimation of the FRP due to the outwelling infrared which is partially absorbed by the aerosols, as well as provide a further uplifting energy source due to the semi-direct effect (Tao et al., 2012; Guo et al., 2019). In other words, the assumptions underlying the plume rise model may not be completely relevant or dominant over this region under these conditions.

A second special region, which completely contrasts with Southern Africa is found in Argentina. In this region, a much smaller amount of the total research area is covered in plumes of 1063-pixels or 2.1%. A large amount of the total aerosol (83.8%) exists below 1km, while only a small amount (5.1%) is found above 2km. In this case, the plume rise model achieved its best match globally, with a large amount (92.2%) found below 1km and a small amount (0.35%) found above 2km.

Furthermore, the loadings of CO and NO_2 are both considerably low as compared to other regions studied in this work. It is under these relatively lesser polluted conditions, where the fires are fewer and/or less intense, where a lower amount of total material is being burned on a per day basis of time over the total surface area burning, or where the meteorology and the vertical thermodynamic structure of the atmosphere are more uniform, that the plume rise model can achieve its best results (Table 4, Fig 6 and Fig S6), and thus that the plume rise model is reasonable to use in such a region. Although it is still obvious that even in this best result case, that the plume rise model is fundamentally biased towards the aerosol vertical distribution being too low, especially the amount into the free troposphere.

As we have observed, the simple plume rise models based on Briggs, 1965, are useful under specific circumstances. This is especially the case when the atmosphere is relatively stable, the total loading of pollutants is not too large (i.e. there is fewer fire masking and less of the semi-direct effect to contend with), and where the density of fires is lower (and hence there is less overall buoyancy changing the atmosphere's dynamics). On top of this, more flat and uniform areas are less likely to have local convection, further leading to an improvement of the effectiveness of the simple plume rise model. It is for these many reasons why we find that the simple plume rise model does not provide an ideal fit over many regions, and for this reason, we propose a simple statistical model as an alternative.

3.3 Regression Model Applied to MISR, OMI, MOPITT and Meteorological Measurements

Since plume rise models rely solely on information related to fire intensity and meteorological conditions in order to compute an aerosol injection height, we want to build a relationship that also includes the net effects of pollutants as well. Therefore, we introduce and globally apply seven different combinations of relationships between FRP, Wind, CO, NO_2 and injection height Eq.1-7. Different combinations of CO and NO_2 are applied to the linear regression model. CO and NO_2 are independently mixed with the meteorological terms in Eq.4 and Eq.5, while they are jointly mixed together with the meteorological terms in Eq.1. A non-linear weighted variable of NO_2/CO is mixed on its own with the meteorological variables in Eq.6, while it is mixed with either one of CO and NO_2 in Eq.2 and Eq.3. The reason for this is that there is a significant physical relevance for determining how much NO_2 is emitted per unit of CO, which is a strong function of the fire temperature as well as Oxygen availability. This set of models is capable of providing a clear relationship between the response of either or both of CO and NO_2. Such an approach allows for us to examine the strengths and weaknesses of each combination in terms of the spatial-temporal distribution of the measured heights, as well as the contribution to the absolute magnitude.

The regression model solely containing NO_2 is an approximation of the concept that the heat of the biomass burning should have an important role to play in terms of the plume height. Furthermore, using NO_2 in this way helps to get around the inherent underestimation of FRP. The regression model solely containing the CO is a proxy for the concept that the mass of biomass burned should make an important contribution towards the plume height. Inclusion of the CO term is also a way to get around the underapproximation of the total burned area, or of any significant contribution from underground burning.

The average statistical error and average statistical correlation (coefficient of determination, R^2) between the datasets used to determine the best-fit coefficients for α, β, γ, δ and ε are displayed in Table 2. While a comparison of the time series of the region-averaged injection height was made over all 14 regions, only those regions passing a level of quality control as described below are retained. First, different linear combinations are evaluated for their correlation against the MISR measurements, with an optimal combination selected and considered to be a success only if $R^2>0.2$ and the $P<0.05$. Furthermore, we compare the modeled average injection height in an absolute sense to the measured values, and retain the data if the difference is smaller than 0.25km. Based on these results, the best-fit model-predicted injection height and the measured averaged injection height were found to be reasonable only at 8 different sites.

In general, when CO or NO_2 or both are included in these different combinations for these regions, the normalized coefficients of CO and NO_2 have a larger value than the respective normalized coefficients of FRP or wind speed. This means that when these variables occur simultaneously, the contaminants have a stronger influence on the final injection height of the plume. This is found to especially be the case in regions which have higher loadings of pollution. The regression model with the non-linear combination of the two is a proxy for the argument that it is the ratio of the heat to the total biomass burned that is an essential physical consideration to take into effect. Furthermore, this final case provides some weight to the concept that a small change in the vertical column concentration may have a stronger than linear effect, as is evidenced by (Ichoku et al., 2008; Zhu et al., 2018), such as in terms of absorbing aerosols in the vertical column altering the ultimate vertical distribution.

Deleted: (which are themselves produced more so under hot or oxygen starved conditions)

This comparison also is found to be valid in regions which in general are less polluted. For example, even in relatively clean Central Canada, the linear combination of NO_2 and the ratio of NO_2 and CO produces the best fit, with the coefficient of NO_2 being roughly an order of magnitude larger (at $3.2x10^3$) as compared to the coefficients of FRP and Wind (which are respectively a magnitude of order smaller, at $3.3x10^2$ and $-2.3x10^2$).

Due to the fact that NO_2 and CO have very different lifetimes in the atmosphere, a fire-based source is expected to have a high level of both CO and NO_2 close to its source, which decays as one heads away in space from the source. This decay should be a function of the wind direction as well, as both the CO and NO_2 upwind will not have a significant source, but downwind the CO will have a significant source, as shown in Fig. 5. We find that our results are consistent with this theory. First, we have found that the regions that have the highest NO_2 at the same time as the MISR measurements are made, also have a very strong overlap well with the locations of the MISR plume heights. We further determine this to be true for every year on a year-by-year basis (Fig S1). Second, we find that the higher values of CO match well with the year-to-year locations of MISR fires (or downwind thereof) at most of the sites, including in Alaska, Central Canada, Central Siberia, East Europe, East Siberia, Northern Southeast Asia, Siberia and North China, and South America. As expected, there greater smearing away from the source regions. As expected, this is due to the fact that the lifetime of CO is much greater.

Following these ideas, the idea of characterizing the by the ratio of NO_2/CO is found to nicely separate the data into three different groups, based on the bands generated by the central 80% of each respective region's NO_2/CO pdf. Group 1 consisting

of Siberia and North China & Central Canada, has a NO_2/CO range from $1x10^{-4}$ to $9x10^{-4}$. Group 2 consisting of the remaining regions, has a NO_2/CO range from $2x10^{-4}$ to 15 $x10^{-4}$ to $20x10^{-4}$. Group 3 consisting of South America, has a NO_2/CO range from 6 $x10^{-4}$ to $43x10^{-4}$. This strong differentiation is consistent with the ratio of NO_2/CO representing a physical meaning, but being a single, continuous variable connected with the temperature of the burning, the wetness of the burning material, the latent heat flux, and the type and amount of biomass being burned.

Furthermore, in terms of changes in time, a climatology of CO should be slightly higher due to the added emissions from the fires, but the NO_2 should be much larger than the climatology, since there is little to no retention in the air, as demonstrated in Table 1. To account for this, we have also looked at the difference between the fire times and the long-term climatology. Over regions which are urban and hence contributing randomly to the variance, we expect the differences to be smaller than due to the fires, and this is observed clearly as well. On top of this, the NO_2 column loading and the ratio of the NO_2/CO column measurements over only the selected grids which have available of FRP measurements, and over the larger regions as given in Fig. 5 are found to generally be consistent, with the ratio found to be more so (Table S2). This indicates the NO_2/CO column ratio over the fire regions tends to be consistent with the fire plumes as a whole, and is not found to be significantly influenced by urban sources of NO_2, which would lead to a vastly faster chemical titration of NO_2 compared to CO. All of these results are also shown to be consistent with recent work (Cohen, 2014; Lin et al., 2014; Lin et al., 2020a), showing that the characteristics of the spatial-temporal variability of fires is quite different from that of urban areas, and has a much higher variability both week-to-week and inter-annually.

Deleted: These

3.4 Comparison between the Plume Rise Model and the Regression Model

The results in Table 3 indicate that inclusion of either one of CO and NO_2 or in some cases both, always provides a better fit to the measured vertical heights when using the regression aerosol height rise model, as compared with those model cases where the loadings of the gasses are excluded. In addition, the fit is better over a larger number of regions (8 regions versus 5 regions), details are shown in Fig. S3. What we observe is that the regression model does relatively better in regions which are more polluted, while the plume rise model does relatively better only in regions which have very low amounts of burning in terms of FRP. A detailed look at the day by day values from the MISR measurements of aerosol height, the regression model of aerosol height, and the plume rise model are given in Fig. 3.

As shown in Fig. 3 there are three regions where both modeling approaches work well. In West Siberia, the regression model shows more stability than plume rise model, with the results more narrowly concentrated around 1000m. Furthermore, the results are mostly found within the range of the measured variation. The plume rise models results are also relatively stable, although more dispersed in general than the regression model. Overall the RMS is 0.47 between the measured values and the regression model, while it is 0.67km between the measured values and the plume rise model. A similar set of results is found in Alaska, with the RMS for the regression modeling being 0.88km and that of the plume rise model being 0.77km. The major

difference here is that the plume rise model results have a variance higher than that of the measurements (SD of 0.91km for the regression model and 3.03km for the plume rise model). In the case of Central Canada, although both modeling approaches have a decent fit, there is a clear difference between their overall performance. In general, the results of the plume rise model (1.73km) are biased significantly lower than both the measurements (1.97km) and the regression model (2.13km), while there is little bias between the measurements and the regression model. To make this point clear, only roughly 7.9% of the measured results are outside of 1 standard deviation from the measured mean, while 50% of the plume rise model results and 43% of the regression model results are found to be outside of the 1 standard deviation from the measured mean. Note that this is the sight which has the highest RMS error and still yields a successful fit for both modeling approaches. Details are given in Fig. S4.

In some of the more highly polluted regions, the regression model showed a decent performance, while the plume rise model did not. The overall goodness of the fit of the regression model is reasonable in the cases of South America, Siberia and North China, Northern Southeast Asia, and Northern Australia. This is because these areas emit large amounts of CO and NO_2, in some cases solely during the biomass burning season, and in other cases due to a combination of biomass burning and urban sources. Overall in these more polluted regions, the regression model is found to have little bias (respectively -0.02km, -0.20km, -0.22km, and 0.15km), which helps to establish the predictive ability of using the gas loadings in terms of predicting the vertical distribution of the aerosol heights.

Although the vertical distribution of aerosol cannot be successfully simulated at all sites by using the regression model approach, at the sites where it provides a reasonable fit, it seems to do better than the plume rise model approach. This is further found to be true in the case where the data at the high end of the NO_2/CO ratio profile are considered. This improvement is found in terms of both the bias and the RMS under all conditions, and even more so at the respective top and bottom 10% of each respective range of NO_2/CO ratio, in which the subset of regression model heights performs much better than the respective plume rise model heights when compared with the MISR height distribution (Figure S7).

These findings are consistent with real true world conditions, where there is a significant impact of co-emitted aerosols and/or heat, and these results with the NO_2/CO ratio would hint that higher burning temperature conditions, or fewer oxygen limited conditions, may be important driving forces. These changes either directly alter the heating throughout the profile as well as indirectly introduce a negative bias on measurements of the FRP below. No matter the underlying specific reasons, overall, we find that the regression model approach yields at least as good if not a more precise representation of the plume rise height as compared with the simple plume rise model. However, combining the two approaches yields the best overall result, since there are some locations in which each approach is better than the other approach.

What is most important to note is that in some of the regions, none of these simple approaches work. This is particularly so for when the measured distribution of the aerosol heights is when there is a diverse set of sources. For example, in Africa there are significant sources from biomass burning, as well as from rapid urbanization and burning over many different land use types and under many different types of conditions. Another potential problem occurs when there may be a significant

Deleted: high values of the three respective NO_2/CO ratio bands…

Deleted: . Under

amount of smoke which has been transported from another region, such as the exchange of smoke between the Maritime Continent and Northern Australia. Furthermore, both approaches will not tend to work well under conditions in which the atmosphere is not highly stable, or has a high variation in weather conditions. Under these conditions, a more complex modeling approach and the improvement of measured fire data.

3.5 Comparison between MISR and the three Models

A comparison between the overall performance of the plume rise model, the regression model, and MERRA leads to a few conclusions (Table 3). First of all, where the regression model exists, it reproduces the MISR height better than both the plume rise model and MERRA. This includes over regions where the overall RMS error is very low such as Eastern Siberia and South America, as well as regions where the overall RMS error is large, such as Central Canada. This is true including over regions in the Arctic as well as in the tropics. Secondly, over the regions in which the regression model does not exist, MERRA provides a better reproduction of the MISR height than the plume rise model in all cases, except for over Argentina. Perhaps this is true because of the fact that although MERRA uses data assimilation and a plume rise model type of code built in, the sharp height rise of the Andes Mountains and high cloud cover over this region lead to challenges that the global MERRA model cannot handle well. The second possible explanation is that the overall height of the plume is very low over Argentina and the local meteorology and FRP values are quite similar, which play to the plume rise model's strengths.

Furthermore, comparing the performance of the plume rise model, the regression model, and MERRA at different percentiles of height leads to additional conclusions (Table 4). On one hand, the regression model is the only one which does not have an obvious bias versus MISR measurements, with the regression model sometimes overapproximating and other times underapproximating different geographic locations at different height levels. In fact, the results at the median and 70% height levels are an excellent fit for 4 of the 8 different regions. On the other hand, both the plume rise model and MERRA have obvious biases. The plume rise model is almost always too low, with the only exception being its ability to model 6 of the 14 regions reasonably well at the 10% height level (i.e. the bottom of the plume). However, in the case where the 10% level is higher than other cases, such as a very narrow distribution, the plume rise model still dos a poor job. MERRA is almost always too high, with it performing best at only South Africa and East Europe. Furthermore, the results from the plume rise model tend to also be narrower than the data, while the results from MERRA tend to be broader than the data. The results of MERRA being broad, as demonstrated clearly in Fig. 4, are not due to a high inter-annual variability, which actually barely exists in the MERRA dataset as compared with the regression model and MISR, but instead due to too much aerosol being found too high in the atmosphere, as well as too much aerosol being found at the surface.

The MISR data, regardless of the region, shows some amount of inter-annual variability. This ranges from a minimum over East Siberia and Siberia and North China, to a maximum over Central Canada and Northern Southeast Asia. On the other hand, MERRA shows only a very small variation anywhere, with most of the years exactly the same as each other. The amount

at the surface is always much larger than found in MISR and the amount in the middle free troposphere is also much larger than in MISR. The largest variation in MERRA is found in Central Canada, Alaska, and Northern Australia. All of these are regions which are relatively cloud free and have vast amounts of ground stations, and therefore will have a large amount of the total MERRA model contribution from reanalysis data.

In the case of East Siberia there is only burning observed by MISR in 2 of the 4 years studied here, although these two different years have quite a different distribution. In 2008, the aerosol is limited in height to under 1000m, while in 2010, the aerosol has a peak height at 1000m and a significant fraction up to 2000m. In the case of Siberia and North China, the peak ranges from 800m to 1200m and the maximum ranges from 2200m to 3000m. MERRA shows no burning at all in East Siberia, with a completely flat profile all 4 years, and a consistent burning year to year, with the aerosol all confined to 1000m and below over Siberia and North China. In terms of the regression model, the fact that there is a good fit is supported by Fig. 5. As can be observed, all of the fire data points occur in regions of high CO and the vast majority also occur in regions of high NO_2. In Siberia and Northern China, the findings in both of the years in Fig. 5 lend support, albeit from two different perspectives. The first is that the fires always overlap with regions of high CO, and that in the 2011, one of the major differences is that the region in the middle has low CO and no fires, which were both present and highly polluted in 2008. The NO_2 is always high over the southern region, and is never very high in the central or northern regions, likely due to the intense cold air present in these regions altering the NO_2 chemistry.

Over Central Canada the MISR data shows peaks or sub-peaks at 1000m in 2008, 2800m and 3200m in 2009, 2000m in 2010, and 1000m and 2600m in 2011. In many of these years the amount located in the free troposphere is much larger than the amount in the boundary layer. Yet, even though this is the region in which MERRA has the most inter-annual variability, in all cases, the vast majority of the aerosol is found below 1000m. Furthermore, no peaks or subpeaks are found anywhere above the surface. Finally, MERRA only shows 1 year to be considerably different from the others, whereas the MISR data shows that all 4 years are quite different. By looking at Fig. 3, we can see that the regression model on some days underestimates the plume, on some days overestimates the plume, and on some days is nearly perfect. There is no bias, and the fact that it is able to capture the range of values over all 4 years indicates that the performance is not only better on average, but as well at capturing the inter-annual variation over this region. This finding is further supported by Fig. 5, where all of the MISR fire points in Central Canada in 2010 are found in high CO pixels, and most of the MISR fire points are also found in high NO_2 pixels. This demonstrates that the vast majority of the MISR plumes are local in nature and actively connected with the ground (due to the short lifetime of NO_2), are in relatively cloud-free regions where these remotely sensed platforms will work, but not necessarily MODIS which may be blocked by the high AOD levels, while also being in regions which are clearly heavily polluted by CO during these times, but are not normally so.

The MISR measurements over Northern Southeast Asia show the majority under 1000m but a second peak around 2500m in 2008, the peak at 2500m and a large amount up to 3200m in 2009, the peak was spread from 500m to 2500m in 2010, and

peaks at 1000m, 1200m, and 2200m in 2011. This huge amount of inter-annual variability is not at all captured by MERRA, which is consistent with other recent findings over this area of the world demonstrating that many products based on MODIS tend to have problems (i.e. Cohen 2014, Cohen et al., 2018). However, the regression model performs well over this region as over all of the years, with measurements again showing an unbiased representation in all 4 years of the height, with some days high, other days low, and some days nearly perfect. This is in part demonstrated clearly in Fig. 3 and Fig. 5 by the fact that the MISR fire points occur over the highest loadings of CO and NO_2 found among any region, anywhere else in the world, as observed in this study.

In terms of the magnitudes of the vertical temperature gradient (dT/dz) and the vertical wind speed at the surface, we have not found any correlation or relationship between the cases in which the regression model performs better or worse. Even considering those cases in which there are extremely atypical values in these variables, such as positive temperature gradients (i.e. an unstable atmosphere), or negative temperature gradients which are more negative than the -9.8 K/km rate which is the pure dry air thermodynamic limit (i.e. extreme stabilization due to intense aerosol/cloud cooling), as observed in Fig. 6. This provides a further piece of support to the idea that the regression model works well under conditions where there is some local non-linear forcing in the system which is not being taken into account, whether it is a coupled chemical, aerosol dynamical/size, radiative-dynamic, thermodynamic, or direct/semi-direct/indirect type of aerosol effect, all of which are being accounted for to some degree by the loadings of NO_2 and CO, but which are missed by the model underlying the meteorological reanalysis data (e.g. Cohen et al., 2011; Wang et al., 2009).

However, it does seem that under the conditions where the regression model was not able to be formed, that there are some important differences in terms specifically of the vertical temperature gradient variable. In specific, in the cases in which the value of dT/dz is either more negative than -9 K/km or positive, that the MERRA results are far better than those from the plume rise model, as compared to not under those conditions. However, such cases only account for 15% or fewer of the total cases observed in this study, and therefore do not play an outsized role.

4 Conclusions

This work quantifies the measured values of the aerosol vertical distribution over biomass burning areas of the Earth on a daily basis from January 2008 through June 2011. We find that there is a significant amount of total aerosol which reaches the free troposphere, as well as large amounts which are not uniformly distributed throughout the boundary layer, both of which are not readily explained by first order theoretical approximations and present-day community-standard models.

To address these issues, we introduce a new approach, based on remotely sensed measurements of fire properties, wind, and column loadings of NO_2 from OMI and CO from MOPITT to constraining the aerosol heights over different geographic regions. This approach is based on the physical concept that the emissions of aerosols and the height to which they rise should

be related to other co-emitted species like NO_2 and CO and the co-emitted heat, which is also a function of the ratios of NO_2 and CO produced by the burning. Our results are compared against both the measured MISR height values as well as basic plume rise model computations using the same fire radiative power and meteorological datasets.

Our results indicate that our new method reproduced the measured values significantly better over much of the world in terms of reproducing the measured vertical distribution as compared with the simpler plume rise approach. In specific, we find that applying the plume rise model leads to a model underestimation of the measured MISR heights overall, whereas our approach, where it works, does not exhibit such a bias. This finding is consistent with the fact that FRP is underestimated globally, in part due to clouds and aerosols, and in part due to sampling and other issues. We also find that the plume rise model tends to be too narrowly confined compared with the regression model and the modeled results. However, the plume rise model does better in terms of reproducing the aerosol injection height when it is solely contained and well mixed within the atmospheric boundary layer, but for higher altitudes, the model capability is poor. The average underestimation of the plume rise model injection height is 33%. On the other hand, the regression model has an overall improved the accuracy of the measured results, in particularly doing a better job reproducing results in the free troposphere. The regression model is also more widely applicable around the globe, with the number or regions successfully simulated increasing from five to eight. As we have demonstrated, the impact of NO_2 (as a proxy for the burning temperature) is always essential, and the impact of CO (as a proxy for the total biomass burned) is usually essential as well. We further have shown that the simplest regression model, the approximation of the plume rise model, never yields the best fit to the data.

In specific, we find that the plume rise model works well in regions which are not frequently cloud covered during the local biomass burning seasons, in particularly so over non-tropical forested regions. In specific, the plume rise model has its greatest successes in Alaska (RMS error of 0.77km for the regression approach versus 0.88km for the plume rise model approach), Argentina (the regression model approach does not succeed versus and RMS error of 0.40km for the plume rise model approach), and Western Siberia (RMS error of 0.47km for the regression approach versus 0.67km for the plume rise model approach). In most of the other parts of the world, the regression model approach is much better at reproducing the vertical distribution than the plume rise model, even including some major extreme events including the release of aerosols into the stratosphere, and tends to do so with a reasonably lower RMS error and low standard deviation.

One of the major advantages of the regression model approach is that it is more capable of picking up those cases where aerosols are lofted into the lower free troposphere, and another advantage stems from its ability to reproduce better those cases where the near surface is clean, but the upper part of the boundary layer is polluted. In the cases of Eastern Siberia and Amazon South America, we find that the regression model performs reasonably well, while the plume rise model does not succeed. In the case of Northern Australia, the regression model is capable of reproducing the aerosol height with a relatively reasonable set of statistics, although the measurements in this region are found to be very unique; sometimes the plume is mainly concentrated in the lower free troposphere and is local in nature, while other times it is found in the upper troposphere and

lower stratosphere, in which case it is thought to be transported from the Maritime Continent. We also find that the regression model works well in two other special cases. The first is the case of Siberia and Northern China, where there is a considerably large amount of local urban pollution which is mixed into the biomass burning plumes. The second is the case of Northern Southeast Asia, where there are both large amounts of local pollution as well as considerable issues with extensive cloud cover.

Our results show clearly that where we can successfully form a regression model, that it performs better than both the plume rise model and MERRA. The specific forms of the regression model that are the best are those which have NO_2 or a combination of NO_2 and CO (in particular when the non-linear term NO_2/CO is considered). These results are consistent with our hypothesis and literature review that show new forms of non-linearity relating plume rise height to factors influencing buoyancy, radiative transfer, and energy transfer in-situ, and/or biases in remotely sensed measurements of FRP and land-surface products are important. Such are not considered in the present generation of plume rise models (including the global-scale models underlying MERRA). In the cases where we cannot form a regression model, we find that MERRA performs better than the plume rise model everywhere, except for Argentina, which has a unique high mountain just upwind in the Andes, coupled with a very low overall height, all of which are disadvantages for the models underlying MERRA. In general, this shows that improved model complexity and data assimilation doe produce a better result, as expected.

We propose the results as a first step of a new approach to parameterization that my help us to move forward in terms of improving our ability to reproduce heights of fire plumes for regional and global scale modeling and analysis studies over many different periods of time. We believe that our sample dataset is currently not sufficiently long to form an ideal fit, and hence thought that excluding data to self-compare was not an ideal use of the very limited resources we had. We do hope that as more new datasets are released, the community will have access to more relevant input data, and as more MISR plume height data is released, the community will have more access to better understand the vertical distribution of height.

Based on these results, including over those regions where none of the results yield a satisfactory response, we have come up with a list of recommendations for how to improve the reproduction of the vertical aerosol distribution in the future. First, improving the accuracy of FRP measurements, especially so under cloud and heavily polluted conditions. Secondly, improving the ability of simple models to compensate for the impact of local-scale radiative forcings, deep convection, aerosol-radiation interactions and aerosol-cloud interactions. Thirdly, the finding that the NO_2/CO ratio is extremely important in terms of matching the vertical distribution works to address the larger community issue of flaming versus smoldering in a more smooth and precise way, opening the possibility of a new continuum approach to consider burning wetness, temperature, and heat. Based on our overall results, we believe that an improvement can be made to the current generation of GCMs, atmospheric chemical transport models, and remote sensing inversions, all of which depend on a more precise knowledge of the aerosol vertical distribution.

Author Contributions

Shuo Wang: data curation, formal analysis, investigation, software, visualization, writing – original draft.

Jason Blake Cohen: conceptualization, funding acquisition, investigation, methodology, project administration, resources, supervision, validation, writing – original draft, review & editing.

Chuyong Lin: data curation, investigation, software.

Weizhi Deng: software, visualization.

Code/Data availability: All processed data, results, and codes are freely available for download at https://doi.org/10.6084/m9.figshare.10252526.v1 and https://doi.org/10.6084/m9.figshare.12386135.v1

Conflict of Interest: The authors declare that they have no conflict of interest.

Acknowledgements

We would like to acknowledge the PIs of the MISR, MOPITT, and OMI instruments for providing the remote sensing measurements, and the NCEP and MERRA2 reanalysis project for providing the meteorology and hydrophobic black carbon measurements. MISR data was obtained from https://misr.jpl.nasa.gov/getData/accessData/, MOPITT data was obtained from https://eosweb.larc.nasa.gov/datapool. OMI data was obtained from https://disc.gsfc.nasa.gov/mirador-guide?tree=project&project=OMI, NCEP data was obtained from https://www.esrl.noaa.gov/psd/data/gridded/data.ncep.reanalysis.html, and MERRA data was obtained from https://disc.gsfc.nasa.gov/datacollection/M2I3NVAER_5.12.4.html. The work was supported by the Chinese National Young Thousand Talents Program (Project 41180002), the Chinese National Natural Science Foundation (Project 41030028), and the Guangdong Provincial Young Talent Support Fund (Project 42150003).

References

Achtemeier, G. L., Goodrick, S. A., Liu, Y., Garcia-Menendez, F., Hu. Y., and Odman, M. T.: Modeling Smoke Plume-Rise and Dispersion from Southern United States Prescribed Burns with Daysmoke, Atmosphere, 2, 358-388, doi:10.3390/atmos2030358, 2011.

Boersma, K.F., Eskes, H.J., Veefkind, J.P., Brinksma, E.J., Van Der A, R.J., Sneep, M., Van Den Oord, G.H.J., Levelt, P.F., Stammes, P., Gleason, J.F., and Bucsela, E.J.: Near- real time retrieval of tropospheric NO_2 from OMI, Atmos. Chem. Phys., 7, 2103–2118, doi:10.5194/acp-7-2103-2007, 2007

Briggs, G. A.: A plume rise model compared with observations. J. Air Pollut. Con. Assoc., 15, 433–438, doi:10.1080/00022470.1965.10468404, 1965.

Buchard, V., A. M. da Silva, P. R. Colarco, A. Darmenov, C. A. Randles, R. Govindaraju, O. Torres, J. Campbell, and R. Spurr (2015), Using the OMI aerosol index and absorption aerosol optical depth to evaluate the NASA MERRA Aerosol Reanalysis, Atmos. Chem. Phys., 15(10), 5743-5760, doi: 10.5194/acp-15-5743-2015.

Chew, B. N., Campbell, J. R., Salinas, S. V., Chang, C., W., Reid, J. S., Welton, E. J., and Liew, S. C.: Aerosol particle vertical distributions and optical properties over Singapore, Atmos. Environ., 79, 599–613, doi:10.1016/j.atmosenv.2013.06.026, 2013.

Cohen, J. B. and Prinn, R. G.: Development of a fast, urban chemistry metamodel for inclusion in global models, Atmos. Chem. Phys., 11, 7629–7656, doi:10.5194/acp-11- 7629-2011, 2011.

Cohen, J. B.: Quantifying the occurrence and magnitude of the Southeast Asian fire climatology, Environ. Res. Lett., 9, 114018, doi:10.1088/1748-9326/9/11/114018, 2014.
Cohen, J. B. and Wang, C.: Estimating global black carbon emissions using a top-down Kalman Filter approach, J. Geophys. Res.-Atmos., 119, 307–323, doi:10.1002/2013JD019912, 2014.
Cohen, J. B., Lecoeur, E., and Hui Loong Ng, D.: Decadal-scale relationship between measurements of aerosols, land-use change, and fire over Southeast Asia, Atmos. Chem. Phys., 17, 721-743, doi:10.5194/acp-17-721-2017, 2017.
Cohen, J. B., Hui Loong Ng, D., Lim, A. W. L., and Xin R. C. J.: Vertical distribution of aerosols over the Maritime Continent during El Niño, Atmos. Chem. Phys., 18, 7095-7108, doi: 10.5194/acp-18-7095-2018, 2018.
Damoah, R., Spichtinger, N., Servranckx, R., Fromm, M., Eloranta, E. W., Razenkov, I. A., James, P., Shulski, M., Forster, C., and Stohl, A.: A case study of pyro-convection using transport model and remote sensing data, Atmos. Chem. Phys., 6, 173– 185, doi:10.5194/acp-6-173-2006, 2006.
Deeter, M.N., Edwards, D.P., Francis, G.L., Gille, J.C., Martinez-Alonso, S., Worden, H.M., Sweeney, C., 2017. A climate-scale satellite record for carbon monoxide: the MO- PITT version 7 product. Atmos. Meas. Tech., 1–34. doi:10.5194/ amt-2017-71, 2017.
Dewitt, H. and Gasore, J.: Seasonal and diurnal variability in O3, black carbon, and CO measured at the Rwanda Climate Observatory, Atmos. Chem. Phys., 19, 2063-2078, doi:10.5194/acp-19-2063-2019, 2019.
Flower V. J. B. and Kahn R. A.: Assessing the altitude and dispersion of volcanic plumes using MISR multi-angle imaging from space: Sixteen years of volcanic activity in the Kamchatka Peninsula, Russia. J. Volcanol. Geotherm. Res., 337 (May1), 1-15, doi: /10.1016/j.jvolgeores.2017.03.010, 2017
Freitas, S. R., Longo, K. M., Chatfield, R., Latham, D., Silva Dias, M. A. F., Andreae, M. O., Prins, E., Santos, J. C., Gielow, R., and Carvalho Jr., J. A.: Including the sub-grid scale plume rise of vegetation fires in low resolution atmospheric transport models, Atmos. Chem. Phys., 7, 3385–3398, doi:10.5194/acp- 7-3385-2007, 2007.
Field, R. D., van der Werf, G. R., and Shen S. P. P.: Human amplification of drought-induced biomass burning in Indonesia since 1960, Nat. Geosci., doi:10.1038/ngeo443, 2009.
Freeborn, P. H., Wooster, M. J., Roy, D. P., and Cochrane, M. A.: Quantification of MODIS fire radiative power (FRP) measurement uncertainty for use in satellite-based active fire characterization and biomass burning estimation, Geophys. Res. Lett., 41, 1988–1994, doi:10.1002/2013GL59086, 2014.
Generoso, S., Bey, I., Atti, J.-L., and Bron, F.-M.: A satellite- and model-based assessment of the 2003 Russian fires: Impact on the Arctic region, J. Geophys. Res., 112, D15302, doi:10.1029/2006JD008344, 2007.
Giglio, L., Csiszar, I., and Justice, C. O.: Global distribution and seasonality of active fires as observed with the Terra and Aqua Moderate Resolution Imaging Spectroradiometer (MODIS) sensors, J. Geophys. Res.-Biogeo., 111, G02016, doi:10.1029/2005JG000142, 2006.
Gonzalez, L., Val Martin, M., and Kahn, R. A.: Biomass-burning smoke heights over the Amazon observed from space, Atmos. Chem. Phys., 19. 1685-1702. 10.5194/acp-19-1685-2019, 2019.
Grandey, B.S., Rothenberg, D., Avramov, A., Jin, Q., Lee, H.H., Liu, X., Lu, Z., Albani, S., Wang, C., 2018. Effective radiative forcing in the aerosol-climate model CAM5.3- MARC-ARG. Atmos. Chem. Phys. 18, 15783–15810. https://doi.org/10.5194/acp-18- 15783-2018, 2018.
Guo, J., Deng, M., Lee, S. S., Wang, F., Li, Z., Zhai, P., Liu, H., Lv, W., Yao W., and Li X.: Delaying precipitation and lightning by air pollution over the Pearl River Delta. Part I: Observational analyses, J. Geophys. Res., 121, 6472-6488, doi: 10.1002/2015JD023257, 2016.
Guo, J., Li, Y., Cohen, J. B., Li, J., Chen, D., Xu, H., Liu, L., Yin, J., Hu, K., and Zhai, P.: Shift in the temporal trend of boundary layer height trend in China using long-term (1979–2016) radiosonde data. Geophysical Research Letters, 46, 6080-6089, doi:10.1029/2019GL082666, 2019.
Gunturu, U. B.: Aerosol-Cloud interactions: a new perspective in precipitation enhancement, 2010.
Ichoku, C., and Ellison, L.: Global top-down smoke-aerosol emissions estimation using satellite fire radiative power measurements, Atmos. Chem. Phys., 14, 6643–6667, doi: 10.5194/acp-14-6643-2014, 2014
Husar, R. B., Prospero, J. M., and Stowe, L. L.: Characterization of tropospheric aerosols over the oceans with the NOAA advanced very high resolution radiometer optical thickness operational product, J. Geophys. Res., 102, 16889–16909, doi:

10.1029/96jd04009, 1997.
Ichoku, C., Giglio, L., Wooster, M., and Remer, L.: Global characterization of biomass-burning patterns using satellite measurements of fire radiative energy, Remote Sens. Environ., 112, 2950–2962, doi: 10.1016/j.rse.2008.02.009, 2008.
Jost, H., Drdla, K., Stohl, A., Pfister, L., Loewenstein, M., Lopez, J. P., Hudson, P. K., Murphy, D. M., Cziczo, D. J., Fromm, M., Bui, T. P., Dean-Day, J., Gerbig, C., Mahoney, M. J., Richard, E. C., Spichtinger, N., Pittman, V. J., Weinstock, E. M., Wilson, J. C., and Xueref, I.: In-situ observations of mid-latitude forest fire plumes deep in the stratosphere, Geophys. Res. Lett., 31, L11101, doi:10.1029/2003GL019253, 2004.
Kahn, R. A., Li, W. H., Moroney, C., Diner, D. J., Martonchik, J. V., and Fishbein, E.: Aerosol source plume physical characteristics from space-based multiangle imaging, J. Geophys. Res., 112, D11205, doi:10.1029/2006JD007647, 2007.
Kahn, R. A., Chen, Y., Nelson, D. L., Leung, F. Y., Li, Q., Diner, D. J., and Logan, J. A..: Wildfire smoke injection heights: Two perspectives from space. Geophysical Research Letters, 35(4), 2008.
Kalnay, E., Kanamitsu, M., Kistler, R., Collins, W., Deaven, D., Gandin, L., Iredell, M., Saha, S., White, G., Woollen, J., Zhu, Y., Chelliah, M., Ebisuzaki, W., Higgins, W., Janowiak, J., Mo, K. C., Ropelewski, C., Wang, J., Leetmaa, A., Reynolds, R., Jenne, R., and Joseph, D.: NCEP/NCAR 40-year reanalysis project, Bull. Amer. Meteor Soc., 1996, 77,437-472, doi: 10.1175/1520-0477(1996)077<0437:TNYRP>2.0.CO;2, 1996.
Kauffman, J. B., Steele, M. D., Cummings D. L., and Jaramillo V. J.: Biomass dynamics associated with deforestation, fire, and, conversion to cattle pasture in a Mexican tropical dry forest, For. Ecol. Manage., 176, 1-12, doi: 10.1016/s0378-1127(02)00227-x, 2003.
Kim, D., Wang, C., Ekman, A. M. L., Barth, M. C., and Rasch, P.: Distribution and direct radiative forcing of carbonaceous and sulfate aerosols in an interactive size-resolving aerosol-climate model, J. Geophys. Res., 113, D16309, doi:10.1029/2007JD009756, doi:10.3390/rs5094593, 2008.
Labonne, M., Bréon, F.-M., and Chevallier, F.: Injection height of biomass burning aerosols as seen from a spaceborne lidar, Geophys. Res. Lett., 34, doi:10.1029/2007GL029311, 2007.
Lamsal, L. N., Martin, R. V., Padmanabhan, A., van Donkelaar, A., Zhang, Q., Sioris, C. E., Chance, K., Kurosu, T. P., and Newchurch, M. J.: Application of satellite observations for timely updates to global anthropogenic NOx emission inventories, Geophys. Res. Lett., 38, doi:10.1029/2010GL046476, 2011.
Leung, F. Y. T., Logan, J. A., Park, R., Hyer, E., Kasischke, E., Streets, D., and Yurganov, L.: Impacts of enhanced biomass burning in the boreal forests in 1998 on tropospheric chemistry and the sensitivity of model results to the injection height to emissions, J. Geophys. Res., 112, D10313, doi:10.1029/2006JD008132, 2007.
Levelt, P. F., van den Oord, G. H. J., Dobber, M. R., Malkki, A., Visser, H., de Vries, J., Stammes, P., Lundell, J. O. V., and Saari, H.: The ozone monitoring instrument, Ieee Trans. Geosci. Remote Sens., 44, 1093–1101, doi:Urn:nbn:nl:ui:25-648485, 2006.
Lin, C. Y., Cohen, J. B., Wang, S., and Lan, R. Y.: Application of a combined standard deviation and mean based approach to MOPITT CO column data, and resulting improved representation of biomass burning and urban air pollution sources, Remote Sens. Environ., 241:11720, https://doi.org/10.1016/j.rse.2020.111720, 2020.
Lin, N. H., Sayer, A. M., Wang, S. H., Loftus, A. M., Hsiao, T. C., Sheu, G. R., and Chantara, S.: Interactions between biomass- burning aerosols and clouds over Southeast Asia: Current status, challenges, and perspectives, Environ. Pollut., 195, 292–307, doi: 10.1016/j.envpol.2014.06.036, 2014.
Mims, S. R., Kahn, R. A., Moroney, C. M., Gaitley, B. J., Nelson, D. L., and Garay, M. J.: MISR stereo-heights of grassland fire smoke plumes in Australia, IEEE Trans. Geosci. Remote Sens., 48, 25–35, doi:10.1109/TGRS.2009.2027114, 2010.
Ming, Y., Ramaswamy, V., and Persad, G.: Two opposing effects of absorbing aerosols on global-mean precipitation, Geophys. Res. Lett., 37, L13701, doi:10.1029/2010GL042895, 2010.
Nelson, D. L., Garay M. J., Kahn R. A., and Dunst B. A.: Stereoscopic Height and Wind Retrievals for Aerosol Plumes with the MISR INteractive eXplorer (MINX), Remote Sens., 5, 4593– 4628, doi:10.3390/rs5094593, 2013.
Oanh, N. T. K., Oo, M., Salinas, S. V., Welton, E. J., and Liew, S. C.: Observing and understanding the Southeast Asian aerosol system by remote sensing: An initial review and analysis for the Seven Southeast Asian Studies (7SEAS) program, Atmos. Res., 122, 403–468, 2013.
Paugam, R., Wooster, M., Freitas, S., and Val Martin, M.: A review of approaches to estimate wildfire plume injection height

within large-scale atmospheric chemical transport models. Atmos. Chem. Phys., 16, 907–925, doi:10.5194/acp-16-907-2016, 2016.

Petersen, W. and Rutledge, S.: Regional variability in tropical convection: observations from TRMM, J. Climate, 14, 3566–3586, doi:10.1175/1520-0469(1989)046<0037:OOLFOI>2.0.CO;2, 2001.

Petrenko, M., Kahn, R. A., Chin, M., Soja, A. J., Kucsera, T., and Harshvardhan: The use of satellite-measured aerosol optical depth to constrain biomass burning emissions source strength in the global model GOCART, J. Geophys. Res., doi:10.1029/2012JD017870, 2012.

Pfister, G. G., Wiedinmyer, C., and Emmons, L. K.: Impacts of the fall 2007 California wildfires on surface ozone: Integrating local observations with global model simulations, Geophys. Res. Lett., 35, L19814, doi: 10.1029/2008GL034747, 2008.

Ramanathan V., Ramana M.V., Roberts G., Kim D., Corrigan C., Chung C., and Winker D.: Warming trends in Asia amplified by brown cloud solar absorption. Nature, 448, 575. doi:10.1038/nature06019, 2007.

Reid, J. S., Hyer, E. J., Johnson, R. S., Holben, B. N., Yokelson, R. J., Zhang, J. L., Campbell, J. R., Christopher, S. A., Di Girolamo, L., Giglio, L., Holz, R. E., Kearney, C., Miettinen, J., Reid, E. A., Turk, F. J., Wang, J., Xian, P., Zhao, G., Balasubramanian, R., Chew, B. N., Janjai, S., Lagrosas, N., Lestari, P., Lin, N. H., Mahmud, M., Nguyen, A. X., Norris, B., Randles, C., Da Silva, A., Buchard, V., Colarco, P., Darmenov, A., Govindaraju, R., Smirnov, A., Holben, B., Ferrare, R., Hair, J.: The MERRA-2 aerosol reanalysis, 1980 onward. Part I: system description and data assimilation evaluation. J. Clim. 30, 6823–6850. 2017.

Rogers, R. R., Hostetler, C. A., Hair, J. W., Ferrare, R. A., Liu, Z., Obland, M. D., Harper, D. B., Cook, A. L., Powell, K. A., Vaughan, M. A., and Winker, D. M.: Assessment of the CALIPSO Lidar 532 nm attenuated backscatter calibration using the NASA LaRC airborne High Spectral Resolution Lidar, Atmos. Chem. Phys., 11, 1295–1311, doi:10.5194/acp-11-1295-2011, 2011.

Steinfeld, J. H. and Pandis, S. N.: Atmospheric chemistry and physics: from air pollution to climate change, Environment, Phys. Today, 40, 26-26, doi:10.1063/1.882420, 2006.

Singh, N., Banerjee, T., Raju, M. P., Deboudt, K., Sorek-Hamer, M., Singh, R. S., and Mall R. K.: Aerosol chemistry, transport, and climatic implications during extreme biomass burning emissions over the Indo-Gangetic Plain, Atmos. Chem. Phys., 18, 14197-14215, doi:10.5194/acp-18-14197-2018, 2018

Spracklen, D. V., Mickley, L. J., Logan, J. A., Hudman, R. C., Yevich, R., Flannigan, M. D., and Westerling A. L.: Impacts of climate change from 2000 to 2050 on wildfire activity and carbonaceous aerosol concentrations in the western United States, J. Geophys. Res.,114, D20301, doi:10.1029/2008JD010966, 2009.

Tao, W.-K., Chen, J.-P., Li, Z., Wang, C., and Zhang, C.: Impact of aerosols on convective clouds and precipitation, Rev. Geophys., 50, RG2001, doi:10.1029/2011RG000369, 2012.

Tosca, M. G., Randerson, J. T., Zender, C. S., Nelson, D. L., Diner, D. J., and Logan, J. A.: Dynamics of fire plumes and smoke clouds associated with peat and deforestation fires in Indonesia, J. Geophys. Res., 116, D08207, doi:10.1029/2010JD015148, 2011.

Trentmann, J., Luderer, G., Winterrath, T., Fromm, M. D., Servranckx, R., Textor, C., Herzog, M., Graf, H.-F., and Andreae, M. O.: Modeling of biomass smoke injection into the lower stratosphere by a large forest fire (Part I): reference simulation, Atmos. Chem. Phys., 6, 5247–5260, doi:10.5194/acp-6- 5247-2006, 2006.

Tsigaridis, K., Daskalakis, N., Kanakidou, M., Adams, P. J., Artaxo, P., Bahadur, R., Balkanski, Y., Bauer, S. E., Bellouin, N., Benedetti, A., Bergman, T., Berntsen, T. K., Beukes, J. P., Bian, H., Carslaw, K. S., Chin, M., Curci, G., Diehl, T., Easter, R. C., Ghan, S. J., Gong, S. L., Hodzic, A., Hoyle, C. R., Iversen, T., Jathar, S., Jimenez, J. L., Kaiser, J. W., Kirkevåg, A., Koch, D., Kokkola, H., Lee, Y. H., Lin, G., Liu, X., Luo, G., Ma, X., Mann, G. W., Mihalopoulos, N., Morcrette, J.-J., Müller, J.-F., Myhre, G., Myriokefalitakis, S., Ng, N. L., O'Donnell, D., Penner, J. E., Pozzoli, L., Pringle, K. J., Russell, L. M., Schulz, M., Sciare, J., Seland, Ø., Shindell, D. T., Sillman, S., Skeie, R. B., Spracklen, D., Stavrakou, T., Steenrod, S. D., Takemura, T., Tiitta, P., Tilmes, S., Tost, H., van Noije, T., van Zyl, P. G., von Salzen, K., Yu, F., Wang, Z., Wang, Z., Zaveri, R. A., Zhang, H., Zhang, K., Zhang, Q., and Zhang, X.: The AeroCom evaluation and intercomparison of organic aerosol in global models, Atmos. Chem. Phys., 14, 10845–10895, doi:10.5194/acp-14- 10845-2014, 2014.

Turquety, S., Logan, J. A., Jacob, D. J., Hudman, R. C., Leung, F. Y., Heald, C. L., Yantosca, R. M., Wu, S., Emmons, L. K.,

Edwards, D. P., and Sachse, G. W.: Inventory of boreal fire emissions for North America in 2004: Importance of peat burning and pyroconvective injection, J. Geophys. Res.-Atmos., 112, D12S03, doi:10.1029/2006JD007281, 2007.

Urbanski, S.: Wildland fire emissions, carbon, and climate: Emission factors, Forest Ecol. Manage., 317, 51–60, doi: 10.1016/j.foreco.2013.05.045, 2014.

Vernon, C. J., Bolt, R., Canty, T., and Kahn, R. A.: The impact of MISR-derived injection height initialization on wild- fire and volcanic plume dispersion in the HYSPLIT model, Atmos. Meas. Tech., 11, 6289–6307, doi:10.5194/amt-11-6289-2018, 2018.

Val Martin, M., Logan, J. A., Kahn, R. A., Leung, F. Y., Nelson, D. L., and Diner, D. J.: Smoke injection heights from fires in North America: analysis of 5 years of satellite observations, Atmos. Chem. Phys., 10, 1491–1510, doi: 10.5194/acp-10-1491-2010, 2010.

Val Martin, M., Kahn, R. A., Logan, J. A., Paugam, R., Wooster, M., and Ichoku, C.: Space-based observational constraints for 1- D fire smoke plume-rise models, J. Geophys. Res.-Atmos., 117, doi.:10.1029/2012JD018370, 2012.

Val Martin, M., Kahn, R. A., and Tosca, M.: A Global Analysis of Wildfire Smoke Injection Heights Derived from Space-Based Multi-Angle Imaging, Remote Sens., 10, 1609, doi: 10.3390/rs10101609, 2018.

Winker, D. M., Tackett, J. L., Getzewich, B. J., Liu, Z., Vaughan, M. A., and Rogers, R. R.: The global 3-D distribution of tropospheric aerosols as characterized by CALIOP, Atmos. Chem. Phys., 13, 3345–3361, doi:10.5194/acp-13-3345-2013, 2013.

Worden, H.M., Deeter, M.N., Edwards, D.P., Gille, J.C., Drummond, J.R., and Nedelec, P.: Observations of near-surface carbon monoxide from space using MOPITT multispectral retrievals, J. Geophys. Res.: Atmos., 115, D18, 27, doi:10.1029/2010JD014242, 2010.

Yu, P. F., Toon, O. B., Bardeen, C. G., Zhu, Y. Q., Rosenlof, K. H., Portmann, R. W., Thornberry, T. D., Gao, R. S., Davis, S. M., Wolf, E. T., Gouw, J., Peterson, D. A., Fromm, M. D., and Robock, A.: Black carbon lofts wildfire smoke high into the stratosphere to form a persistent plume, Science, 365, 587–590, doi: 10.1126/science.aax1748, 2019.

Zhu, L., Martin, M. V., Gatti, L. V., Kahn, R., Hecobian, A., and Fischer, E. V.: Development and implementation of a new biomass burning emissions injection height scheme (BBEIH v1.0) for the GEOS-Chem model (v9-01-01), Geosci. Model Dev., 11(10): 4103-4116, doi:10.5194/gmd-11-4103-2018, 2018

Figures

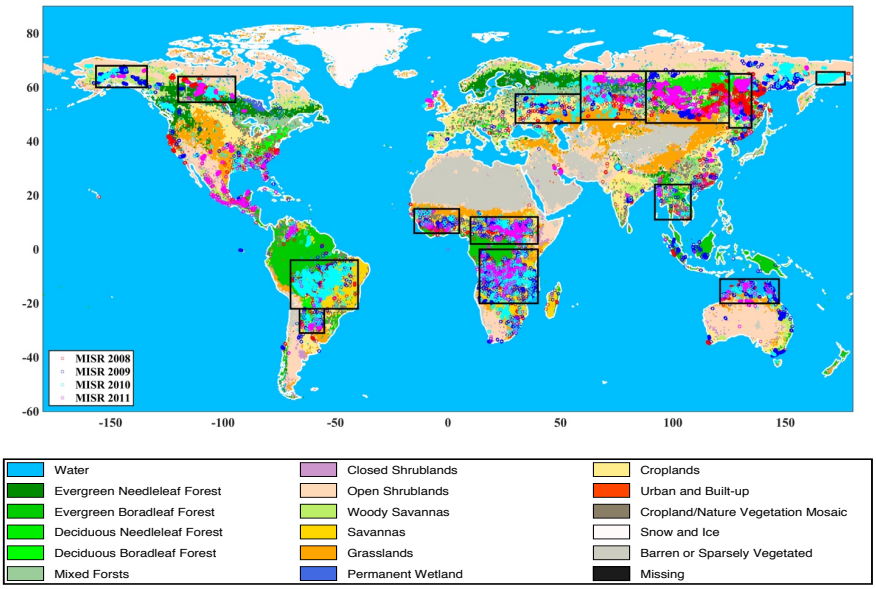

Figure 1: Land surface type at each of the daily MISR measurements from January 2008 to June 2011. Each dot corresponds to an individual aerosol plume, with different colors representing different years.

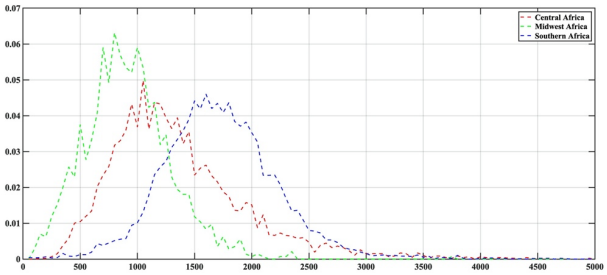

(a)

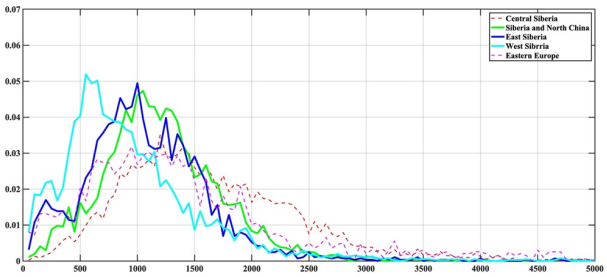

(b)

(c)

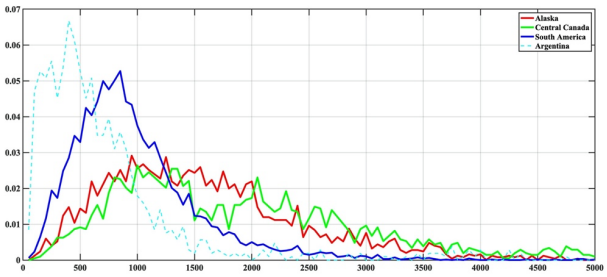

(d)

Figure 2: PDFs of all daily MISR plume height measurements from January 2008 through June 2011 (which are 5000m or less) over each of the following geographic regions: (a) Africa, (b) Eurasian High Latitudes, (c) Tropical Asia, and (d) the Americas. Solid lines correspond to regions which have a successful regression model, while dashed lines are regions which do not.

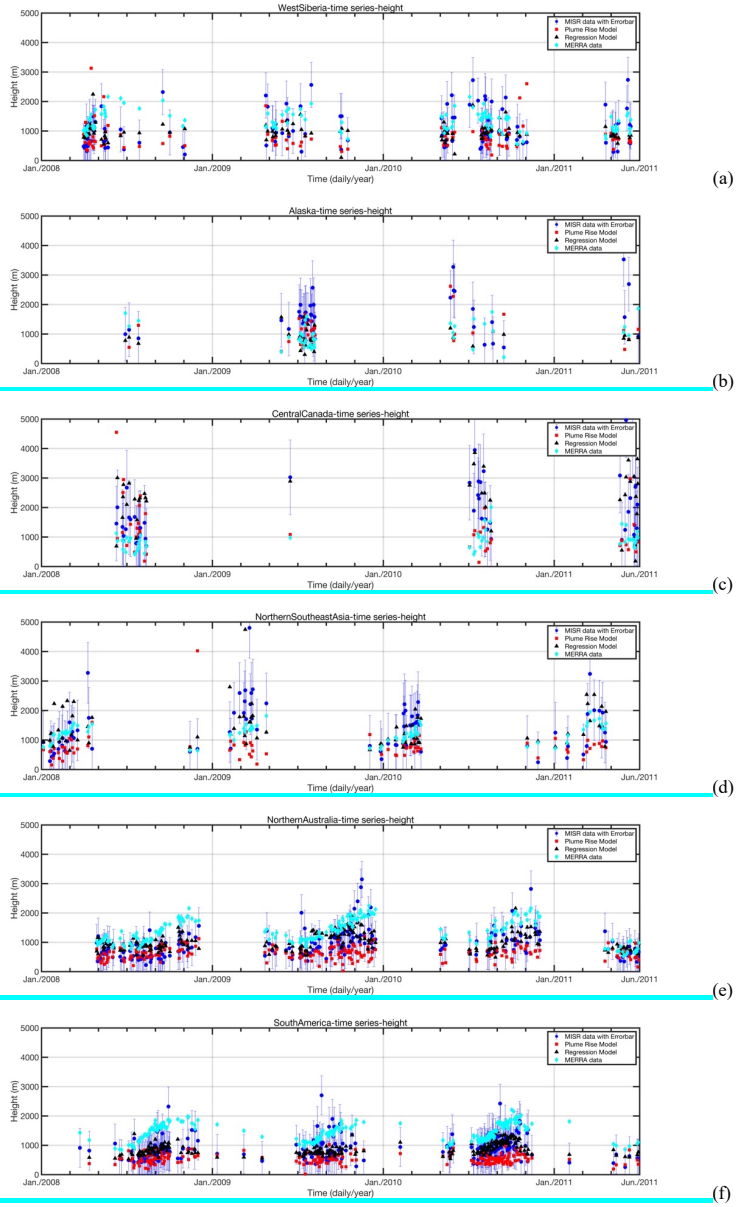

Figure 3: Time series of daily average measured MISR aerosol height (blue circles [m]) with an error bar corresponding to 1 sigma (blue bars [m]), the plume rise model height (red squares [m]), the regression model height (black squares [m]), and the MERRA hydrophobic black carbon mean height (blue diamonds [m]). Part (a) corresponds to West Siberia, part (b) to Alaska, part (c) to Central Canada, part (d) to Northern Southeast Asia, part (e) to Northern Australia, and part (f) to South America. Missing data points are due to a lack of MISR measurements and/or measurements of regression model predictor(s).

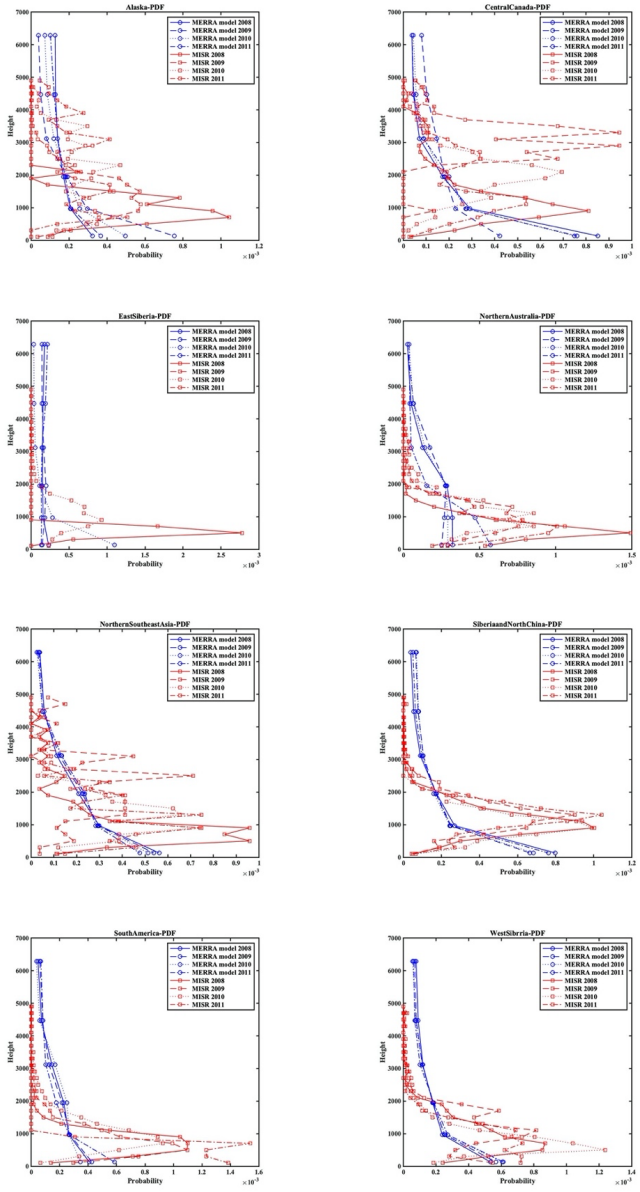

Figure 4: PDF of the vertical distribution of MISR heights (red lines for 2008, red dashes for 2009, red dots for 2010, and red dash-dots for 2011) and MERRA hydrophobic black carbon heights (blue lines, color scheme the same as for MISR). These plots are only over regions in which the regression model applies.

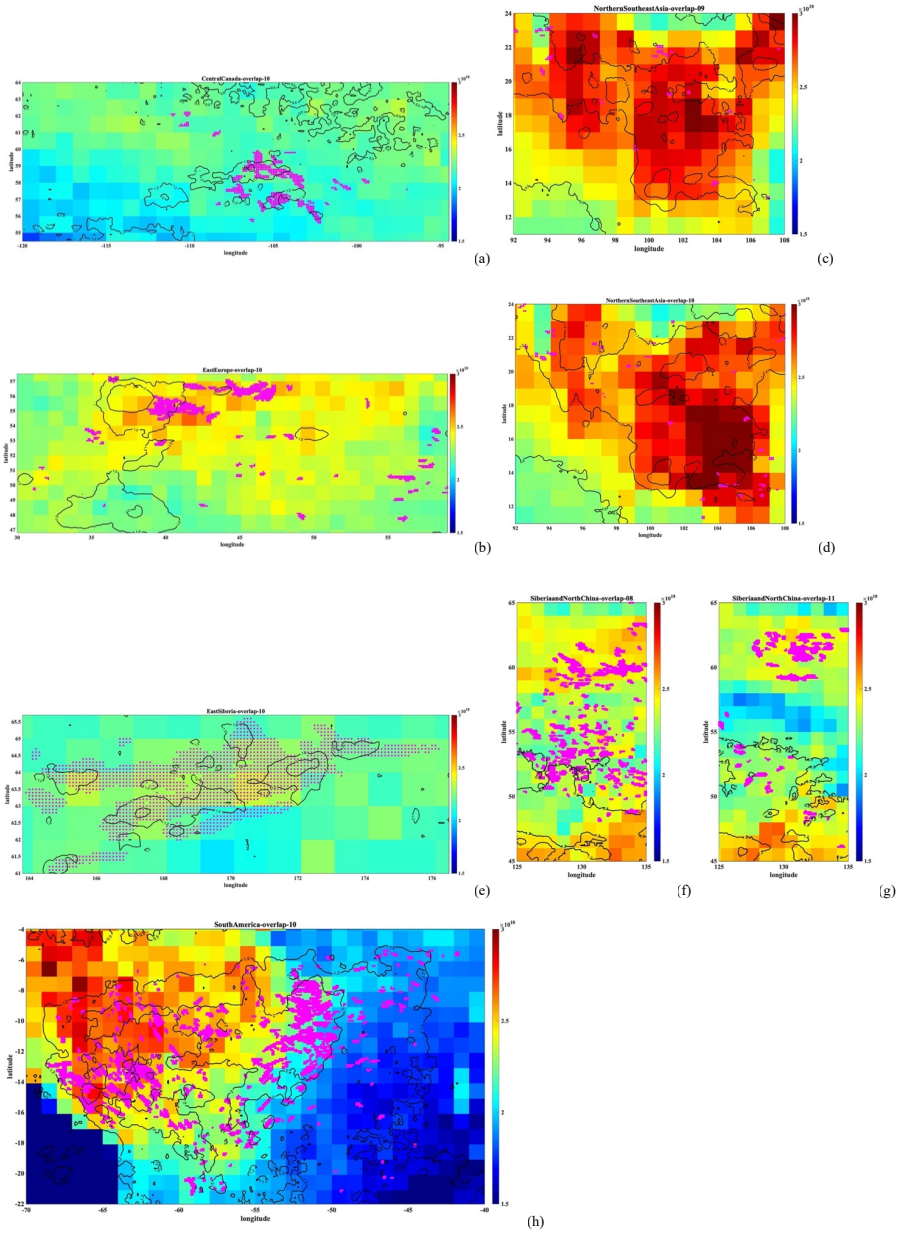

Figure 5: Spatial distribution of annual fires (magenta dots), mean NO_2 column loading on days where there are fires (black isopleths [$*10^{15}$ mol/cm^2]), and mean CO column loading on days where there are fires (Colorbar, mol/cm^2). The corresponding regions are: (a) 2010 Central Canada, (b) 2010 East Europe, (c) 2009 and (d) 2010 Northern Southeast Asia, (e) 2010 East Siberia, (f) 2008 and (g) 2011 Siberia and Northern China, and (h) 2010 South America.

Deleted: compilation of all MISR

Deleted: OMI

Deleted: MOPITT

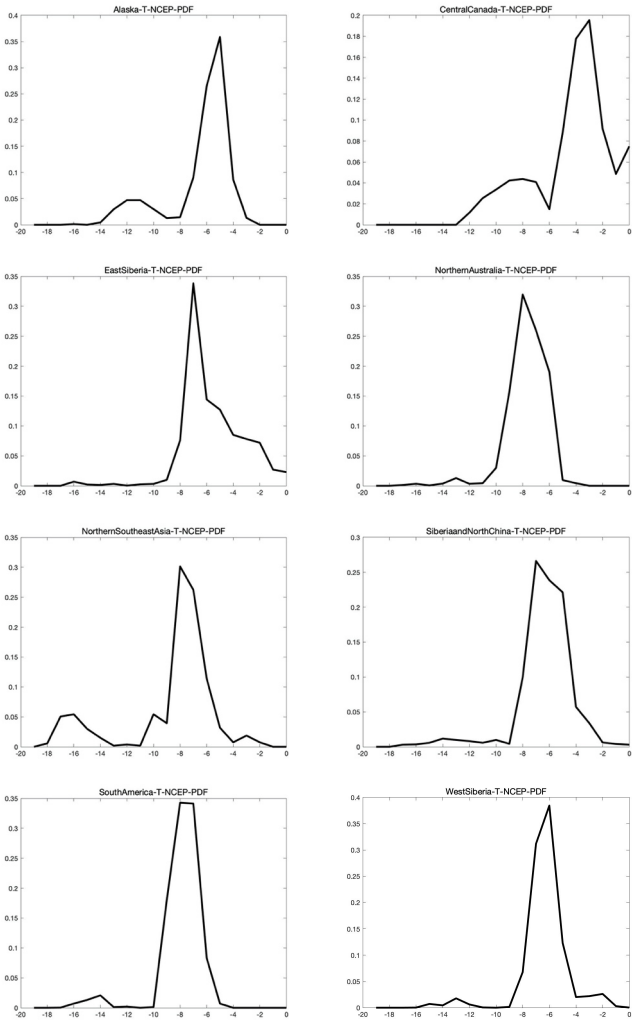

Figure 6: PDFs of the NCEP reanalysis vertical temperature gradient d[K]/d[km] over the locations and days that contain MISR plumes. The 8 regions over which the regression model are valid are shown.

Tables

	C_{NO2} (entire box)	C_{NO2} (fire only)	C_{CO} (entire box)	C_{CO} (fire only)
Central Africa	1.36e+15	3.24e+15	2.24e+18	2.49e+18
Midwest Africa	1.20e+15	3.12e+15	2.45e+18	2.60e+18
Southern Africa	1.40e+15	3.60e+15	1.94e+18	2.24e+18
Central Siberia	8.63e+14	1.11e+15	2.04e+18	2.78e+18
Siberia and Northern China	1.36e+15	1.13e+15	2.31e+18	2.90e+18
Eastern Siberia	4.74e+14	1.50e+15	2.25e+18	2.38e+18
Western Siberia	1.21e+15	1.70e+15	2.20e+18	2.52e+18
Northern Southeast Asia	1.43e+15	2.94e+15	2.58e+18	3.09e+18
Northern Australia	7.53e+14	1.73e+15	1.50e+18	1.73e+18
Alaska	7.63e+14	1.46e+15	2.07e+18	2.12e+18
Central Canada	5.98e+14	1.02e+15	2.13e+18	2.15e+18
South America	1.16e+15	6.36e+15	1.78e+18	3.08e+18
Argentina	1.22e+15	1.32e+15	1.51e+18	1.62e+18
Eastern Europe	1.70e+15	1.81e+15	2.25e+18	2.79e+18

Table 1: Statistical summary of measured column loadings of OMI NO_2 [molecule/cm^2] and MOPITT CO [molecule/cm^2] averaged from January 2008 to June 2011, over each entire boxed region (entire box) as well as the subset in space and time containing active fires (fire only).

Region	α	β	γ	δ	ε	R^2
Siberia and North China	110	318	NaN	300	-518	0.26
East Siberia	-163	-657	1480	NaN	437	0.41
West Siberia	241	196	-221	NaN	-263	0.22
Northern Southeast Asia	367	139	912	NaN	355	0.31
Northern Australia	211	-4	NaN	1820	-1580	0.24
Alaska	163	18	2674	-892	NaN	0.37
Central Canada	-232	334	NaN	3190	-1970	0.50
South America	226	57	314	NaN	8	0.30

Table 2: Best fit values for the various coefficients of the regression models based on Eq.1-7. NaN refers to predictors which are not associated with the given model.

	MISR data	Plume Rise Model	RMS	Regression Model	RMS	MERRA Data	RMS
Central Africa	1.36 *(0.80)*	0.59 *(0.22)*	0.95	NAN	NAN	**1.72 *(0.50)***	**0.56**
Midwest Africa	0.90 *(0.42)*	0.60 *(0.23)*	0.47	NAN	NAN	**1.42 *(0.45)***	**0.41**
South Africa	1.71 *(0.56)*	0.58 *(0.23)*	1.18	NAN	NAN	**1.64 *(0.50)***	**0.44**
Central Siberia	1.64 *(0.90)*	0.87 *(0.89)*	1.01	NAN	NAN	**2.11 (*1.01*)**	**0.66**
Siberia and North China	1.27 *(0.97)*	0.80*(0.64)*	0.69	**1.07 (*0.30*)**	**0.42**	2.06 *(1.20)*	0.52
Eastern Siberia	1.12 *(1.00)*	0.68*(0.34)*	0.52	**1.32 (*0.65*)**	**0.35**	3.13 *(1.09)*	0.68
West Siberia	0.95 *(0.77)*	0.79 (*0.95)*	0.67	**0.97 (*0.29*)**	**0.47**	1.71 *(0.84)*	0.53
Northern Southeast Asia	1.57 *(1.03)*	0.73*(0.38)*	1.04	**1.42 (*0.51*)**	**0.68**	1.40 *(0.63)*	0.75
Northern Australia	0.90 *(0.62)*	0.64*(0.29)*	0.57	**1.12 (*0.38*)**	**0.52**	1.69 *(0.63)*	0.59
Alaska	1.57 *(0.91)*	1.39 *(3.03)*	0.88	**1.26 (*0.45*)**	**0.77**	2.48 *(0.97)*	1.01
Central Canada	1.97 *(1.26)*	1.73 (*2.19*)	1.36	**2.13 (*1.72*)**	**1.20**	2.54 *(1.17)*	1.36
South America	0.97 *(0.66)*	0.50*(0.21)*	0.52	**0.95 (*0.22*)**	**0.37**	1.92 *(0.91)*	0.60
Argentina	0.69 *(0.70)*	**0.65 (*0.25*)**	**0.40**	NAN	NAN	1.30 *(0.49)*	0.52
Eastern Europe	1.41 *(1.05)*	1.27 (*2.67)*	0.85	NAN	NAN	**1.15 *(0.59)***	**0.65**

Table 3: Statistics of measured MISR plume heights and (standard deviations) (2nd column [km]) using all available daily data from Jan 2008 to Jun 2011; plume rise model heights and (standard deviations) (3rd column [km]); RMS error between the MISR plume heights and plume rise model heights (4th column [km]); regression model heights and (standard deviations) (5th column [km]); RMS error between the MISR plume heights and regression model heights (6th column [km]); MERRA daily mean hydrophobic black carbon heights and (standard deviations) (7th column [km]); and finally the RMS error between the MISR plume heights and MERRA daily hydrophobic black carbon heights (8th column [km]). NaN indicates that the regression model failed over the respective region. The model type with the lowest RMS error over each region is given in "Bold".

	MISR 10%	MISR 30%	MISR 50%	MISR 70%	MISR 90%	PRM 10%	PRM 30%	PRM 50%	PRM 70%	PRM 90%
Central Africa	0.70	0.99	1.22	1.53	2.10	0.33	0.47	0.57	0.68	0.85
Midwest Africa	0.43	0.69	0.87	1.05	1.37	0.30	0.49	0.60	0.70	0.85
South Africa	1.12	1.44	1.67	1.92	2.31	0.32	0.46	0.56	0.67	0.84
Central Siberia	0.75	1.15	1.48	1.93	2.62	0.38	0.59	0.74	0.91	1.27
Siberia and North China	0.58	0.92	1.15	1.41	1.88	0.38	0.55	0.68	0.84	1.24
East Siberia	0.41	0.77	1.00	1.29	1.69	0.36	0.49	0.62	0.78	0.97
West Siberia	0.28	0.56	0.79	1.09	1.71	0.38	0.52	0.62	0.76	1.14
Northern Southeast Asia	0.48	0.87	1.35	1.91	3.03	0.32	0.55	0.71	0.84	1.10
Northern Australia	0.28	0.56	0.79	1.09	1.52	0.34	0.49	0.63	0.75	0.93
Alaska	0.59	1.02	1.43	1.88	2.78	0.52	0.83	1.00	1.20	1.56
Central Canada	0.72	1.16	1.73	2.36	3.51	0.51	0.74	0.98	1.68	3.04
South America	0.38	0.64	0.85	1.11	1.65	0.26	0.39	0.50	0.60	0.77
Argentina	0.14	0.34	0.51	0.75	1.26	0.34	0.50	0.63	0.76	0.97
East Europe	0.44	0.85	1.19	1.60	2.63	0.47	0.64	0.82	1.08	1.97

(a)

	RM 10%	RM 30%	RM 50%	RM 70%	RM 90%	MERRA 10%	MERRA 30%	MERRA 50%	MERRA 70%	MERRA 90%
Central Africa	nan	nan	nan	nan	nan	1.08	1.47	1.71	1.96	2.33
Midwest Africa	nan	nan	nan	nan	nan	0.87	1.18	1.40	1.62	1.99
South Africa	nan	nan	nan	nan	nan	1.01	1.35	1.62	1.90	2.29
Central Siberia	nan	nan	nan	nan	nan	0.87	1.51	1.99	2.53	3.49
Siberia and North China	0.89	1.02	1.13	1.27	1.50	0.55	1.27	1.92	2.64	3.74
East Siberia	0.95	1.41	1.66	1.88	2.66	1.72	2.57	3.14	3.72	4.56
West Siberia	0.72	0.84	0.93	1.03	1.22	0.67	1.22	1.63	2.06	2.81
Northern Southeast Asia	0.81	1.00	1.20	1.69	2.64	0.68	0.99	1.29	1.65	2.29
Northern Australia	0.71	0.87	1.04	1.25	1.53	0.91	1.29	1.64	2.01	2.52
Alaska	0.30	0.80	0.82	0.85	1.35	1.25	1.94	2.43	2.94	3.76
Central Canada	0.80	2.01	2.28	2.78	4.59	1.02	1.81	2.49	3.22	4.13
South America	0.71	0.86	0.98	1.11	1.36	0.90	1.38	1.77	2.22	3.19
Argentina	nan	nan	nan	nan	nan	0.70	1.01	1.25	1.52	1.94
East Europe	nan	nan	nan	nan	nan	0.43	0.78	1.09	1.40	1.90

(b)

Table 4: Statistics of the 10%, 30%, median, 70% and 90% percentile heights [km] of MISR heights and plume rise model heights (a), and regression model heights and MERRA heights (b). NaN refers to regions where there is no regression model result.